Nature Communications

https://doi.org/10.1038/s41467-026-70257-x

Article in Press

sRNA centered signaling activates nitrate respiration and enhances *Cronobacter sakazakii* virulence in host environments

Received: 6 July 2025

Accepted: 23 February 2026

Cite this article as: Li, X., Sun, H., Yang, X. *et al.* sRNA centered signaling activates nitrate respiration and enhances *Cronobacter sakazakii* virulence in host environments. *Nat Commun* (2026). https://doi.org/10.1038/s41467-026-70257-x

Xiaoya Li, Hao Sun, Xinyuan Yang, Liying Feng, Yuanyuan Niu, Binbin Xiang, Jingliang Qin, Jiake Wang, Zhengang Li, Lu Wang, Lu Feng, Lei Wang & Bin Liu

sRNA Centered Signaling Activates Nitrate Respiration and Enhances *Cronobacter sakazakii* Virulence in Host Environments

Xiaoya Li[a,#], Hao Sun[a,b,#], Xinyuan Yang[a], Liying Feng[a], Yuanyuan Niu[a], Binbin Xiang[a], Jingliang Qin[a], Jiake Wang[a], Zhengang Li[a], Lu Wang[c], Lu Feng[a,b,d], Lei Wang[a,b,d,*] and Bin Liu[a,b,d,*]

[a] National Key Laboratory of Intelligent Tracking and Forecasting for Infectious Diseases, TEDA Institute of Biological Sciences and Biotechnology, Nankai University, Tianjin 300457, China.

[b] The Key Laboratory of Molecular Microbiology and Technology, Ministry of Education, Nankai University, Tianjin 300071, China.

[c] College of Basic Medical Science, Three Gorges University, Hubei 443000, China.

[d] Nankai International Advanced Research Institute, Shenzhen, China.

[#] These authors contributed equally: Xiaoya Li and Hao Sun.

[*] To whom correspondence may be addressed. E-mail: liubin1981@nankai.edu.cn or wanglei@nankai.edu.cn.

Abstract

Cronobacter sakazakii is an important neonatal pathogen frequently associated with powdered infant formula. However, the mechanisms by which *C. sakazakii* adapts to the host environment and establishes systemic dissemination remain poorly understood. Here, we reveal a signal transduction pathway centered on a novel sRNA, CsrN, which facilitates *C. sakazakii* in utilizing nitrate respiration in response to oxygen-limited environments within the host, thereby enhancing its virulence *in vivo*. *C. sakazakii* infection triggers an inflammatory response, leading to the accumulation of host-derived nitrate, a key alternative electron acceptor. The expression of CsrN is induced under anaerobic conditions via the ArcAB two-component regulation system. CsrN subsequently enhances the expression of the *narGHJI* operon, which encodes a nitrate reductase complex. This promotes the colonization of *C. sakazakii* in the gastrointestinal tract and benefits its survival within macrophages, ultimately leading to increased systemic bacterial dissemination and virulence in the host. We show that administration of tungstate, a specific inhibitor of nitrate respiration, significantly attenuates *C. sakazakii* virulence in animal experiments. This work provides novel insights into the survival and pathogenicity mechanisms employed by *C. sakazakii* in host environments and suggests nitrate respiration as a potential therapeutic target for combating *C. sakazakii* infections.

Keywords: neonatal pathogen; *Cronobacter sakazakii*; nitrate respiration; small RNA; systemic dissemination.

Introduction

Cronobacter spp, are Gram-negative, facultatively anaerobic bacteria recognized as opportunistic pathogens that pose a serious threat to neonates and immunocompromised infants [1,2]. Among them, *Cronobacter sakazakii* is the most clinically significant species, frequently associated with both outbreaks and sporadic cases worldwide [3]. Infection caused by *C. sakazakii* can result in life-threatening conditions, such as bacteremia, sepsis, necrotizing enterocolitis, meningitis and brain abscesses, with reported mortality rate reaching up to 80% based on epidemiological data [4,5]. Survivors often suffer from long-term neurological complications, including quadriplegia, hydrocephalus and delayed neural development [6]. Although *C. sakazakii* is ubiquitous in the environment, its primary transmission source is reconstituted powdered infant formula (PIF) [7]. This is largely attributed to the bacterium's remarkable resistance to desiccation, osmotic stress, and high temperature [1,2,6,8]. Furthermore, the emergence of multi-drug resistant *C. sakazakii* renders the effective treatment more challenging, which has been regarded as an important concern in public health [9].

Beyond reducing contamination risks during PIF production, a comprehensive understanding of the virulence mechanisms of *C. sakazakii* is essential for developing effective preventive and therapeutic strategies. The infection process of *C. sakazakii* typically begins with the colonization of the gastrointestinal tract (GIT) [2]. Several virulence factors contribute to the ability of *C. sakazakii* to adhere to intestinal mucosal surfaces, among which OmpA and OmpX play particularly prominent roles [7]. Following colonization, *C. sakazakii* can translocate into the

bloodstream, where it exhibits systemic persistence by evading immune responses and replicating within macrophages [7,10,11]. Survival within macrophages is an essential step for *C. sakazakii* to establish systemic dissemination, as the pathogen can evade the host immune defense, penetrate the tissue barrier and translocate to the bloodstream, liver, and spleen through macrophages [2,7,12]. Furthermore, *C. sakazakii* is capable of penetrating the blood-brain barrier (BBB) by invading human brain microvascular endothelial cells, ultimately leading to meningitis [7,13].

Adenosine triphosphate (ATP) is essential for bacterial proliferation, serving as the primary energy source for biosynthetic processes. Bacterial cells generate ATP through a series of redox reactions, whereby electrons are transferred from electron donors, such as glucose, to electron acceptors, with oxygen (O_2) being the most efficient due to its high redox potential. This process releases substantial free energy that fuels cellular activities [14]. However, within host environments, bacteria frequently encounters oxygen-limited conditions, which necessitate the use of alternative electron acceptors, such as tetrathionate, nitrate and fumarate [15,16]. The ability to efficiently exploit these alternative respiratory pathways enable pathogens to maximize energy production, thereby facilitating rapid proliferation and competitive advantage over commensal microbes [14]. However, the mechanisms by which *C. sakazakii* adapts to the gut environment and establishes systemic dissemination remain largely unclear.

The process of *C. sakazakii* infection is shaped by a complex array of host environment factors. In bacteria, small RNAs (sRNAs) play crucial roles in regulating gene expression in response to changing environmental conditions [17]. A critical regulatory mechanism employed by

many pathogens involves post-transcriptional modulation via sRNAs, which function by base-pairing with specific mRNA targets to influence processes such as growth, metabolism, cell signaling, and immune evasion [17-19]. Despite their recognized importance in other bacterial pathogens, the specific roles of sRNA in *C. sakazakii* virulence remain largely unexplored.

In this study, we identified a signal transduction pathway that activates nitrate respiration, thereby enhancing the pathogenicity of *C. sakazakii* through an sRNA, CsrN. We found that the expression of CsrN is induced by the ArcAB two-component systems under anaerobic condition. CsrN increases the expression of *narGHJI*, which encodes the nitrate reductase, by directly binding to the 5′ untranslated region (UTR) of *narGHJI* mRNA. Activation of nitrate respiration significantly promotes the survival of *C. sakazakii* in both the gut lumen and macrophages, ultimately facilitating its systemic dissemination within the host. Furthermore, administration of tungsten to neonatal rats significantly attenuated gastrointestinal colonization and systemic dissemination of *C. sakazakii* by inhibiting the molybdenum-cofactor-dependent nitrate respiration pathway. Our results suggest that targeting nitrate respiration may represent a promising therapeutic strategy for combating *C. sakazakii* infection.

Results

CsrN is a small RNA in *C. sakazakii* that is induced during infection

Using publicly available RNA-seq data from *C. sakazakii* ATCC 29544 during its infection of RAW264.7 cells [20], we identified a previously uncharacterized sRNA located in the intergenic region between the genes *yhcB* (inner membrane protein) and *degQ* (HtrA family serine

endoproteases), and named it CsrN (Fig. 1A). Notably, the expression of CsrN was found to be upregulated during infection [20], indicating a potential role in the virulence of *C. sakazakii* (Fig. 1B).

To determine whether CsrN functions as an sRNA in *C. sakazakii* ATCC 29544, we conducted Northern blotting using a CsrN-specific probe. A distinct RNA band was detected in both the wild-type (WT) and the ΔCsrN complemented strain (ΔCsrN+pCsrN), but was absent in the ΔCsrN strain, indicating that CsrN is transcribed from the reverse strand of the *C. sakazakii* ATCC 29544 genome (Fig. 1C). To precisely map the ends of CsrN, we employed 5′ and 3′ rapid amplification of cDNA ends (RACE), which confirmed that CsrN was 181 nt in length, spanning coordinates 608,538 to 608,718 in the genome (Supplementary Fig. 1A). Secondary structure prediction using RNAfold [21] revealed that CsrN consists of six hairpin loops, five interior loops and one multiloop (Fig. 1D).

Given that the RNA chaperone Hfq is often involved in sRNA stability and function [22], we investigated whether CsrN requires Hfq. Northern blotting analysis revealed no significant difference in CsrN expression between Δ*hfq* and WT strains (Supplementary Fig. 1B). Additionally, a rifampicin transcription inhibition assay [22] showed that the degradation rates of CsrN exhibited no significant difference between Δ*hfq* and WT strains, indicating that Hfq does not influence the stability of CsrN (Supplementary Fig. 1C). These results suggest that CsrN is an Hfq-independent sRNA.

A sequence homology search showed that CsrN is present only in *Cronobacter spp*. In order to explore the distribution of CsrN in *C. sakazakii*, we performed a comparative genomics

analysis using 188 publicly available complete *C. sakazakii* genomes (Supplementary Data 1). The results showed that CsrN was present in 97.3% *C. sakazakii* strains (183/188), suggesting the prevalence and importance of CsrN in *C. sakazakii*.

CsrN enhances *C. sakazakii* virulence *in vitro* and *in vivo*

Given the replication within macrophages enables pathogens to establish systemic disease, we infected RAW264.7 cells with *C. sakazakii* to assess whether CsrN contributes the survival of *C. sakazakii* in macrophages. Growth curves analysis showed that WT and ΔCsrN exhibited similar growth rates in monoculture *in vitro* (Supplementary Fig. 2A-B). However, the survival of ΔCsrN within RAW264.7 cells was significantly decreased compared to that of WT and ΔCsrN complemented strains at 1, 4, 24 h post infection (hpi) (Fig. 2A). These results indicate that CsrN promotes the intracellular survival of *C. sakazakii* in macrophages. Meanwhile, we also detected the cytotoxicity in macrophages infected with WT, ΔCsrN or ΔCsrN complemented strain, as measured by LDH release at 1, 4, 24 hpi. The result showed that the ΔCsrN strain was significantly less cytotoxic to macrophages compared to WT strain (Supplementary Fig. 2C). These results indicate that deletion of CsrN in *C. sakazakii* reduces bacterial intracellular survival and cytotoxicity in macrophages.

To investigate the role of CsrN in bacterial pathogenicity *in vivo*, we orally infected 2- to 5-day-old rats with WT, ΔCsrN and ΔCsrN complemented strains. Specimens from the small intestine, colon, blood, liver, and spleen were collected at 48 hpi and plated on the LB agar plate to assess GIT colonization and systemic dissemination. The results showed that rats infected with

ΔCsrN exhibited significant lower bacterial burdens in the small intestine, colon, blood, liver, and spleen compared to those infected with WT and ΔCsrN complemented strains, suggesting that CsrN contributes to both GIT colonization and systemic dissemination of *C. sakazakii* within the host (Fig. 2B). Furthermore, rats infected with ΔCsrN exhibited prolonged survival times compared to those infected with WT and ΔCsrN complemented strains (Fig. 2C). To further validate these findings, we constructed a stable luciferase reporter plasmid using the *frr* promotor and *luxCDABE* operon, following the method described by Kevin Howe [23], and transformed it into WT, ΔCsrN, and ΔCsrN complemented strains, respectively. This allowed us to monitor infection level in rats using live imaging. Bioluminescence imaging (BLI) showed that rats infected with ΔCsrN-Lux exhibited significantly reduced dissemination of bacteria into systemic organs compared with those infected with WT-Lux or ΔCsrN complemented-Lux strain (Fig. 2D). We further investigated the inflammatory factor production and histological damage in the intestines of neonatal rats infected by *C. sakazakii*. The results showed that the levels of IL-6 and TNF-α, as well as histopathology scores, were significantly higher in WT-infected rats than those in ΔCsrN-infected rats (Fig. 2E-F and Supplementary Fig. 2D), indicating that the severity of disease caused by ΔCsrN infection in neonatal rats was significantly decreased compared to that caused by WT infection. Collectively, these results indicate that CsrN plays a critical role in the virulence of *C. sakazakii in vivo*.

CsrN enhances *narGHJI* expression by stabilizing its mRNA

To investigate the molecular mechanism by which CsrN regulates the virulence of *C.*

sakazakii, we compared the transcriptional profiles of WT and ΔCsrN using RNA-seq. A total of 124 differentially expressed genes between the two strains were identified, including 29 genes that were significantly down-regulated and 95 genes that were up-regulated in the absence of CsrN (Fig. 3A, Supplementary Data 2).

KEGG pathway enrichment analysis revealed distinct regulatory patterns in the ΔCsrN strain, with the top five significantly up- and down-regulated pathways further visualized through chord diagrams (Fig. 3B). Based on RNA-seq results, we found that the expression of *narGHJI* operon (Fig. 3C), which encodes a membrane-bound anaerobic nitrate reductase complex [24] related to nitrogen metabolism in KEGG pathways, was significantly down-regulated in ΔCsrN (Fig. 3A-B).

The nitrate reductase complex functions to reduce nitrate to nitrite, a key process in anaerobic nitrate respiration [14]. To confirm that *narGHJI* is regulated by CsrN, we performed qRT-PCR analysis on WT and ΔCsrN grown in LB medium. The results showed a significant reduction in *narGHJI* expression in ΔCsrN compared to WT strain (Fig. 3D), consistent with our RNA-seq data (Fig. 3A-B). Additionally, during macrophage infection, the expression of *narGHJI* in ΔCsrN was also significantly reduced at 1, 4, 24 hpi (Fig. 3E and Supplementary Fig. 3A-B). A similar down-regulation trend was also observed in the small intestine and colon of rats infected with ΔCsrN compared with those infected by WT (Fig. 3F and Supplementary Fig. 3C). These results indicated that CsrN positively regulates the expression of *narGHJI* both *in vitro* and *in vivo*.

To investigate whether CsrN directly regulates the expression of *narGHJI*, we analyzed

potential base-pairing interactions between CsrN and *narGHJI* using IntaRNA [25]. The analysis revealed a 14-nucleotide complementary region between the 5′ UTR of *narGHJI* mRNA (GCGUUACCGUCCCG) and the CsrN sRNA (CGGGACGGCAGCGC), with a 3-nucleotide motif in the CsrN hairpin loop (CGG) that may facilitate the binding (Fig. 3G). Subsequently, we conducted RNA electrophoretic mobility shift assay (REMSA) to test whether there is a direct interaction *in vitro*, using CsrN sRNA and 5′ UTR of *narGHJI* mRNA obtained though *in vitro*-transcription. The results demonstrated that CsrN sRNA binds to the 5′ UTR of *narGHJI* mRNA, as well as to its complementary strand (CsrN+, positive control), in a dose-dependent manner (Fig. 3H and Supplementary Fig. 3D). In contrast, no interaction was observed between the mutant CsrN sRNA ($CsrN^{mut}$, with the binding site CGG mutated to AGC) and 5′ UTR of *narGHJI* mRNA (Fig. 3I), or between CsrN sRNA and a mutant 5′ UTR of *narGHJI* mRNA (5′ UTR^{mut} of *narGHJI*, with the binding site CCG mutated to GCU) (Fig. 3J). However, a direct interaction was observed between the $CsrN^{mut}$ sRNA and 5′ UTR^{mut} of *narGHJI* mRNA (Fig. 3K). These results indicate that CsrN increases the expression of *narGHJI* by directly binding to the 5′ UTR of *narGHJI* mRNA through a specific binding motif in the hairpin loop.

To further confirm the regulatory role of CsrN, we constructed a luciferase reporter plasmid by fusing the promoter and 5′ UTR of *narGHJI* or its mutant (5′ UTR^{mut} of *narGHJI*, with CCG mutated to GCU) with *luxCDABE*. These plasmids were transformed into ΔCsrN to generate strains ΔCsrN *narGHJI-lux* and ΔCsrN *narGHJI*^{mut}-*lux*, respectively. Overexpression of CsrN in ΔCsrN *narGHJI-lux* strain significantly increased luminescence intensity, while overexpression of $CsrN^{mut}$ had no effect (Fig. 3L). In contrast, the luminescence intensity of ΔCsrN *narGHJI*^{mut}-

lux exhibited no significant change upon overexpression of CsrN, but exhibited a significant increase when $CsrN^{mut}$ was overexpressed (Fig. 3M), confirming that CsrN increases the expression of *narGHJI* by directly binding to the 5′ UTR of *narGHJI* mRNA.

To investigate whether CsrN increases the expression of *narGHJI* by influencing its mRNA stability, we performed a rifampicin transcription inhibition assay. The results showed that *narGHJI* mRNA degraded more rapidly in ΔCsrN compared to WT, as evidenced by reduced expression of *narH* and *narJ* in ΔCsrN (Fig. 3N-O), indicating that CsrN enhances the stability of *narGHJI* mRNA. Additionally, the expression of *narH* and *narJ* in Δ*hfq* strain showed no significant difference compared to WT strain (Supplementary Fig. 3E-F). These results demonstrate that CsrN directly binds to the 5′ UTR of *narGHJI* mRNA in an Hfq-independent manner, promoting its expression by stabilizing the mRNA.

narGHJI promotes the pathogenicity of _C. sakazakii_

To investigate the role of *narGHJI* in *C. sakazakii* virulence, we constructed a Δ*narGHJI* mutant strain and a double-knockout strain ΔCsrNΔ*narGHJI*. Growth curve analysis revealed no significant difference in growth rates among WT, Δ*narGHJI* and ΔCsrNΔ*narGHJI* strains when cultured *in vitro* (Supplementary Fig. 4A-B). However, the survival of Δ*narGHJI* in macrophage was significantly reduced compared with that of WT (Fig. 4A). This survival deficiency was restored to WT levels through plasmid complementation (Fig. 4A). It indicates that *narGHJI* benefits the survival of *C. sakazakii* in macrophages. In addition, the survival of ΔCsrNΔ*narGHJI* exhibited no significant difference compared with that of Δ*narGHJI* or

ΔCsrNΔ*narGHJI* complemented with CsrN (ΔCsrNΔ*narGHJI* + pCsrN) strain, indicating that CsrN deletion did not affect the bacterial survival in macrophages in a Δ*narGHJI* background (Fig. 4A and Supplementary Fig. 4C). The analysis of cytotoxicity in macrophages showed that the Δ*narGHJI* strain was significantly less cytotoxic to macrophages compared to WT strain (Supplementary Fig. 4D). These results suggest that deletion of *narGHJI* in *C. sakazakii* reduces bacterial intracellular survival and cytotoxicity in macrophages.

To investigate whether *narGHJI* contributes to systemic dissemination *in vivo*, neonatal rats were orally infected with the WT, Δ*narGHJI*, ΔCsrNΔ*narGHJI* and Δ*narGHJI* complemented strains (Δ*narGHJI*+p*narGHJI*), respectively. The results showed that rats infected with Δ*narGHJI* exhibited significantly lower bacterial burdens in the blood, liver, and spleen compared with those infected with WT or Δ*narGHJI* complemented strain (Fig. 4B). We also evaluated the colonization of Δ*narGHJI* in the small intestine and colon, an environment with limited oxygen [14]. The results revealed that *narGHJI* was essential for the colonization of *C. sakazakii* in the GIT, as rats infected with Δ*narGHJI* exhibited a significantly decreased bacterial burdens in the small intestine and colon compared with those infected with WT or Δ*narGHJI* complemented strain (Fig. 4B). Moreover, rats infected with Δ*narGHJI* exhibited prolonged survival times compared to those infected with WT or Δ*narGHJI* complemented strain (Fig. 4C). BLI analysis also showed that Δ*narGHJI*-Lux exhibited reduced dissemination into systemic organs compared with WT-Lux or Δ*narGHJI* complemented-Lux strain (Fig. 4D). These data indicate that *narGHJI* contributes to the virulence of *C. sakazakii in vivo*. Furthermore, no significant differences in the survival rates were observed among rats infected with

ΔCsrNΔ*narGHJI*, Δ*narGHJI* or ΔCsrNΔ*narGHJI* + pCsrN strain (Fig. 4C and Supplementary Fig. 4E). The bacterial burdens in the blood, liver, spleen, small intestine and colon of rats infected with ΔCsrNΔ*narGHJI* exhibited no significant difference from those in rats infected with Δ*narGHJI* or ΔCsrNΔ*narGHJI* + pCsrN strain, confirming that CsrN's impact on *C. sakazakii* pathogenicity is medicated through *narGHJI* (Fig. 4B and Supplementary Fig. 4F). In addition, we found that the levels of IL-6 and TNF-α, as well as the histopathology scores, in the intestines of neonatal rats infected with WT were significantly higher than those of rats infected with Δ*narGHJI* (Fig. 4E-F and Supplementary Fig. 4G). Collectively, these results showed that *narGHJI* plays a critical role in the pathogenicity of *C. sakazakii* within the host.

Moreover, we showed that the 5′ UTR$^{mut\text{-}nar}$ strain (mutated the binding motif of *narGHJI* 5′ UTR (CCG to GCU) on the chromosome of WT) and CsrN^{mut} strain (mutated the binding motif of CsrN (CGG to AGC) on the chromosome of WT) exhibited significantly reduced survival in macrophage at 1, 4, 24 hpi, as well as markedly attenuated systemic dissemination levels in neonatal rats compared to WT strain (Supplementary Fig. 4H-I). In contrast, the 5′ UTR$^{mut\text{-}nar}$CsrN^{mut} strain, in which the binding motifs in 5′ UTR of *narGHJI* (CCG to GCU) and CsrN (CGG to AGC) were simultaneously mutated on the chromosome of WT, exhibited restored bacterial survival in macrophage and *in vivo* bacterial burdens in neonatal rats comparable to WT level (Supplementary Fig. 4H-I). These results further confirm that CsrN positively regulates *narGHJI* expression through a specific RNA-RNA interaction mediated by its binding motif, thereby promoting *C. sakazakii* survival in macrophages and facilitating systemic dissemination in the host.

Nitrate respiration is essential for the full virulence of *C. sakazakii*

Previous studies have demonstrated that intestinal inflammation can create a nutrient-rich niche that promotes bacterial replication within the host [26]. For instance, *Salmonella* exploits host-derived nitrate and tetrathionate generated during inflammation as alternative electron acceptors to support anaerobic respiration, providing a metabolic advantage over other gut microbes [16,27]. To investigate whether the attenuated virulence observed in Δ*narGHJI* is associated with impaired nitrate respiration, we first measured nitrate levels in the small intestine and colon of *C. sakazakii*-infected rats, as well as in the supernatant of infected macrophage cultures at 1, 4, 24 hpi *in vitro*. Compared to uninfected controls, nitrate levels were significantly elevated in both intestinal tissues and macrophage supernatants following infection (Fig. 5A-B). Then we performed qRT-PCR to analyze the expression of host proinflammatory markers (*Tnf*, *Nos2*) in the small intestine and colon of *C. sakazakii*-infected rats and in *C. sakazakii*-infected macrophages at 1, 4, 24 hpi *in vitro*. Notably, *Nos2* encodes inducible nitric oxide synthases (iNOS), which catalyzes the production of nitric oxide (NO). NO is subsequently oxidized or reacts with reactive oxygen species to form nitrate [28]. We found that the expression of these host proinflammatory genes was significantly increased in infected samples *in vivo* and *in vitro* (Fig. 5C-D). These results indicate that *C. sakazakii* infection induces an inflammatory response, leading to elevated *Nos2* expression and nitrate accumulation within hosts, which may facilitate the growth of *C. sakazakii* through nitrate respiration.

NarK, a nitrate/nitrite transporter, is always highly expressed under anaerobic conditions in

the presence of nitrate and plays a central role in bacterial nitrate uptake [29]. To further confirm the role of nitrate respiration on *C. sakazakii* pathogenicity, we examined the expression of *narGHJI* and *narK* by qRT-PCR in infected macrophages. The results showed that both the expression of *narGHJI* and *narK* in *C. sakazakii* was significantly upregulated in infected macrophages at 1, 4 and 24 hpi, compared with that of bacteria grown in LB medium (Fig. 5E and Supplementary Fig. 5A-B). Then we constructed a Δ*narK* mutant and showed that its survival in macrophages was significantly decreased compared to that of WT strain (Fig. 5F). Additionally, rats infected with Δ*narK* exhibited significantly lower bacterial burdens in the small intestine, colon, blood, liver, and spleen compared with those of WT-infected rats (Fig. 5G). These findings further underscore the essential role of nitrate respiration in *C. sakazakii* survival and systemic dissemination during host infection.

Due to its high redox potential, nitrate serves as a preferred electron acceptor under anaerobic respiration [30]. To investigate its role in *C. sakazakii* growth, we performed bacterial growth experiments under both aerobic and anaerobic conditions, with or without nitrate supplementation. The results showed that the growth of Δ*narGHJI*, Δ*narK*, and WT exhibited no significant difference in aerobic environments, regardless of nitrate supplementation (Supplementary Fig. 5C). However, under anaerobic conditions, the WT strain exhibited significantly enhanced replication compared to the Δ*narGHJI* and Δ*narK* at 1, 4, 24 hours (Fig. 5H), and showed slightly increased growth compared to the ΔCsrN strain, although this difference was not statistically significant (Supplementary Fig. 5D). Moreover, nitrate supplementation significantly promoted the anaerobic growth of both WT and ΔCsrN strains, but

had no significant effect on the growth of Δ*narGHJI* and Δ*narK* strains (Fig. 5H and Supplementary Fig. 5D). Notably, under nitrate-supplemented conditions, the WT strain showed significantly greater growth than ΔCsrN (Supplementary Fig. 5D). Infection assays in macrophages with or without nitrate supplementation demonstrated that nitrate supplementation significantly enhances the intracellular survival of WT and ΔCsrN strains (Fig. 5I and Supplementary Fig. 5E), but had no effect on the survival of either Δ*narGHJI* or Δ*narK* (Fig. 5I). These results indicate that *C. sakazakii* is capable of utilize nitrate as an electron acceptor to support anaerobic respiration, which in turn promotes its survival and proliferation.

ArcAB senses anaerobic condition to enhance *narGHJI* expression via CsrN

To investigate the mechanism through which the expression of CsrN and *narGHJI* is induced within host, we performed a DNA pull-down assay to identify potential regulators binding to the promoter of CsrN. The mass spectrometry result showed that ArcA is a potential regulator that binds to the promoter of CsrN (Supplementary Data 3). ArcA, together with ArcB, forms a two-component regulation system (TCS) that sense changes in oxygen availability and regulate the expression of downstream genes [31]. We showed that the expression of CsrN was significantly decreased in Δ*arcA* mutant compared to WT when grown in LB medium under anaerobic conditions, but there was no significant difference under aerobic conditions (Fig. 6A and Supplementary Fig. 6A). Additionally, the expression of both CsrN and *narGHJI* was significantly decreased in Δ*arcA* mutant compared to the WT strain in infected macrophages which represent an oxygen-limited condition [33] (Fig. 6B and Supplementary Fig. 6B-C),

indicating that ArcA positively regulates CsrN and *narGHJI* expression under anaerobic conditions. Moreover, no significant difference in *narGHJI* expression was observed between ΔCsrN and ΔCsrNΔ*arcA* strains under either aerobic or anaerobic conditions (Fig. 6C and Supplementary Fig. 6D), suggesting that ArcA regulate the expression of *narGHJI* through CsrN. Electrophoretic mobility shift assay (EMSA) showed that phosphorylated ArcA (but not unphosphorylated ArcA) binds to the CsrN promoter in a dose-dependent manner (Fig. 6D). In contrast, ArcA showed no binding to a DNA fragment derived from the *kana* gene (negative control) (Supplementary Fig. 6E). Chromatin immunoprecipitation (ChIP) qPCR demonstrated that the CsrN promoter (P_{CsrN}) was enriched 2.78-fold in the ArcA-ChIP samples compared to the Mock-ChIP samples (Fig. 6E). As a control, no significant enrichment was observed for *rpoS*. These results indicate that ArcA directly activates the expression of CsrN by binding to its promoter.

ArcA, a key regulator of anaerobic responses, enables bacteria to adapt to anaerobic environments [32]. qRT-PCR assays and northern blot analysis were performed to further analyze CsrN expression in *C. sakazakii* cultured aerobically or anaerobically in minimal media. The results showed a significant upregulation of CsrN expression in WT under anaerobic condition compared to aerobic condition (Fig. 6F-G). Consistently, the expression of the *narGHJI*, the downstream target of CsrN, was also significantly elevated under anaerobic conditions compared to aerobic conditions (Fig. 6G). In contrast, no significant difference in the expression of CsrN and *narGHJI* was observed in Δ*arcA* between aerobic and anaerobic conditions (Fig. 6H-I). These results further confirmed that ArcA promotes the expression of CsrN and *narGHJI* under

anaerobic conditions. Furthermore, qRT-PCR assays showed that the CsrN and *narGHJI* expression of *C. sakazakii* in WT-infected rats, were significantly upregulated in the small intestine and colon, in which oxygen availability is limited, compared to that grown in LB medium (Supplementary Fig. 6F-G), in agreement with *in vitro* anaerobic culture data (Fig. 6F-G). However, the expression of CsrN and *narGHJI* in Δ*arcA* in the small intestine and colon of infected rats exhibited no significant difference compared to that grown in LB medium (Supplementary Fig. 6H-I). Previous study reported that the intracellular environment is also oxygen-limited [33], consistent with our observation of elevated expression of CsrN and *narGHJI* in macrophages (Fig. 1B, 5E, and Supplementary Fig. 5A-B). In contrast, when we infected macrophages with Δ*arcA*, the expression of CsrN and *narGHJI* at 1, 4, 24 hpi exhibited no significant difference compared to that of Δ*arcA* grown in LB medium (Supplementary Fig. 6J-L). Moreover, we found that the survival of Δ*arcA* in macrophages and its system dissemination *in vivo* were significantly reduced compared to those of the WT or Δ*arcA* complemented strain (Fig. 6J and Supplementary Fig. 6M). Collectively, these results demonstrate that ArcA functions as an oxygen sensor within the host, activating CsrN expression under anaerobic conditions. This, in turn, leads to the induction of *narGHJI* and promotes nitrate respiration, thereby contributing to the pathogenicity of *C. sakazakii*.

Targeting nitrate respiration to control *C. sakazakii* infection

Bacteria exhibit remarkable metabolic versatility, enabling them to adapt to varying oxygen levels and electron acceptor availability [34]. To evaluate the role of aerobic respiration, anaerobic

respiration, and fermentation on *C. sakazakii* pathogenicity, we constructed mutants in several key metabolic pathways: *cydAB* (encoding cytochrome bd oxidase, a terminal oxidase facilitating aerobic respiration under low-oxygen conditions), *frdABCD* (encoding fumarate reductase, which reduces fumarate as an alternative terminal electron acceptor in anaerobic respiration), *dmsABC* (encoding DMSO reductases involved in DMSO respiration under anaerobic conditions), *adhE* (involved in ethanol fermentation) and *ldhA* (involved in lactate fermentation) strains. Growth curve analysis showed no significant difference in growth between these mutants and WT under both aerobic (Supplementary Fig. 7A-B) and anaerobic conditions (Fig. 7A). Intracellular survival assays showed that the deletion of *cydAB*, *frdABCD*, *dmsABC*, *adhE* or *ldhA* did not influence the survival of *C. sakazakii* in macrophages (Fig. 7B). In addition, infection assays in rats revealed no significant difference in bacterial burdens in the intestine or systemic organs between the mutants and WT (Fig. 7C). These findings suggest that none of the aerobic or anaerobic metabolic pathways, including those governed by *cydAB*, *frdABCD*, *dmsABC*, *adhE*, and *ldhA*, are essential for the virulence of *C. sakazakii*. Instead, these results imply that nitrate respiration is the primary metabolic pathways utilized by *C. sakazakii* to thrive within the host.

Our above results showed that nitrate respiration plays a vital role in the colonization of GIT and systemic dissemination by *C. sakazakii* within the host. Tungstate has been shown to disrupt nitrate respiration in *Enterobacteriaceae* by substituting molybdenum in the molybdopterin cofactor, an essential component of enzymes driving this metabolic pathway [35,36]. We found that the addition of nitrate significantly promoted WT growth under anaerobic conditions. However,

this growth-promoting effect was markedly inhibited by co-supplementation with tungstate (Supplementary Fig. 7C). Notably, in the presence of both nitrate and tungstate, the addition of increasing concentrations of molybdate progressively restored the anaerobic growth of the WT (Supplementary Fig. 7C). In contrast, supplementation with nitrate, tungstate or molybdate had no significant effect on the growth of Δ*narGHJI* under anaerobic conditions (Supplementary Fig. 7D). Additionally, the growth of *C. sakazakii* WT and Δ*narGHJI* showed no significant difference in the presence of tungstate or molybdate under aerobic conditions (Supplementary Fig. 7E). These results indicate that supplementation with tungstate disrupts nitrate respiration of *C. sakazakii*, thereby inhibiting the bacterial growth under anaerobic conditions.

To access whether tungstate treatment would inhibit the infection of *C. sakazakii*, neonatal rats were orally infected with *C. sakazakii* and then treated with tungstate. The results revealed that tungstate treatment significantly reduced *C. sakazakii* burdens in the small intestine, colon, blood, liver, and spleen at 48 hpi compared to untreated rats (Fig. 7D). In contrast, tungstate treatment had no effect on the virulence of Δ*narGHJI in vivo* (Fig. 7E). Meanwhile, we also performed 16S rRNA sequencing on bacterial DNA from the caecal content of tungstate-treated and control rats. The Chao index, Shannon index, and the PCoA based on Bray-Curtis distances showed that tungstate treatment did not significantly alter intestinal bacterial diversity (Supplementary Fig. 7F-G). Moreover, we assessed the relative abundance of the gut microbiota in each group. Consistently, variations at the genus level also showed that tungstate treatment did not alter the overall community structure (Supplementary Fig. 7H-I). The results indicate that tungstate effectively inhibits *C. sakazakii* colonization in the GIT and its systemic dissemination

within the host, without significantly altering the gut microbiota, highlighting targeting nitrate respiration may serve as a promising therapeutic intervention for *C. sakazakii* infections.

Discussion

Nitrate is a preferred electron acceptor due to its high redox potential [37]. Under normal physiological conditions, dietary intake serves as the major source of nitrate. However, during systemic inflammatory responses, such as sepsis or severe gastroenteritis, *Nos2* is highly expressed, leading to elevated production of NO, which is eventually converted to nitrate [16,38]. In the mucosa of the small and large intestine, the lumen-apposed epithelia limits the access of oxygen to the intestinal lumen, resulting in the oxygen availability is limited in the small intestine (~1-6% O_2) and colon (<1% O_2) [14,38,39]. Beyond the gut, intracellular oxygen levels in human macrophages are typically around 1%, even under ambient oxygen conditions [33]. Additionally, during phagocytosis, macrophages produce reactive nitrogen species, such as NO and peroxynitrite ($ONOO^-$), which further inhibit the aerobic respiration of engulfed bacteria [40,41]. In this study, we showed that the anaerobic environment within the host intestine, along with host-driven production of nitrate induced by *C. sakazakii* infection, promotes the pathogen to use nitrate-dependent anaerobic respiration, through an ArcA-CsrN-*narGHJI* regulatory pathway (Fig. 8). This metabolic adaptation not only allows *C. sakazakii* to compete with fermentative gut microbes, but also enhances its survival within macrophages, highlighting a critical strategy for persistence during infection.

C. sakazakii has been found in various foods, including dairy products, meats, drinking water, and dried fish products, highlighting its infectious nature [42,43]. Recent study found that the LysR-type transcriptional regulator, YeiE, promotes the expression of sulfite reductase CysJI which mediates the rapid decrease in sulfite and generation H_2S in *C. sakazakii*, helping the bacterium counteract ROS produced by neutrophils [12]. However, the energy metabolism of *C. sakazakii* within the host remains poorly studied. While aerobic respiration has been reported as essential for the virulence of pathogens, such as *Salmonella enterica*, *Streptococcus agalactiae* and *Staphylococcus aureus*, in systemic disease models [44-46], our study found that deletion of the *cydAB*, which encodes cytochrome bd oxidase, had no significant effect on the virulence of *C. sakazakii* both *in vivo* and *in vitro* (Fig. 7A-C). Previous studies have also demonstrated the crucial roles of anaerobic respiration and associated metabolic pathways in bacterial survival and virulence. For instance, *frdABCD*, which encodes fumarate reductase, facilitates anaerobic respiration and enhances bacterial motility, aiding the survival of bacteria in viscous environments [47]. Similarly, *adhE* is involved in metabolic adaptation under anaerobic conditions and contribute to host cell adhesion in *E. coli* [48]. In addition, the use of alternative electron acceptors such as DMSO and TMAO has been well-characterized in *E. coli* under anoxic conditions [49]. However, *C. sakazakii* lacks TMAO reductase gene in its genome, and blocking other anaerobic metabolism pathways have no effect on its virulence, as demonstrate in our study (Fig. 7B-C). Therefore, we conclude that nitrate respiration is the dominant metabolic pathway utilized by *C. sakazakii* for survival and pathogenicity within the host.

C. sakazakii, an opportunistic foodborne pathogen, has shown a troubling rise in global

outbreak frequency in recent years [50]. Although antimicrobial therapy has long served as the primary therapeutic approach against *C. sakazakii* infection [51], this strategy is being challenged by the emergence of multidrug-resistant strains isolated from both food and clinical samples worldwide [52-54]. Therefore, it is important to develop safe and effective alternative therapeutic strategies for the treatment of severe *C. sakazakii* infection. Our findings reveal that targeted inhibition of nitrate respiration pathways substantially impairs bacterial survival and virulence, suggesting this metabolic pathway as a promising therapeutic target.

C. sakazakii primarily infects newborns, causing life-threatening meningitis and sepsis. While conventional antibiotics can combat bacterial infections, they often indiscriminately disrupt the gut microbiota, eliminating beneficial bacteria that are essential for gut health [55]. This disruption has a profound impact on children's health and their subsequent growth and development [56]. In contrast, tungsten-based treatment specifically targets *C. sakazakii* populations that rely on nitrate respiration under disease conditions. In light of both our work (Supplementary Fig. 7F-I) and prior evidence [57], tungsten appears to have a minimal effect on commensal microbiota, though further validation is warranted. These results suggest that inhibition of bacterial nitrate respiration may offer a precision therapeutic alternative to conventional broad-spectrum antibiotics against the infection of *C. sakazakii*.

Methods

Ethics statement

All animal experiments were conducted in compliance with the guidelines outlined in the Guide

for the Care and Use of Laboratory Animals. All animal studies were conducted according to protocols approved by the Institutional Animal Care Committee of Nankai University (Tianjin, China) and were performed under protocol no. IACUC 2020030501.

Bacterial strains, primers, plasmids and growth conditions

Bacterial strains, plasmids and primers used in this study are provided in Supplementary Table 1 and 2. *C. sakazakii* strain ATCC 29544 spontaneously developed resistance to nalidixic acid was used as the wild-type (WT) strain throughout this study. Mutant strains of *C. sakazakii* were generated using the λ-red recombination system by pKD3 or pKD4 plasmid with chloramphenicol or kanamycin resistance genes [58]. A helper plasmid named pCP20 encoding the FLP recombinases was used to eliminate the antibiotic resistance gene, when required. Complementary plasmids were constructed using pACYC184, and electroporated into corresponding mutant strains. For purification of ArcA-6×His, *arcA* was fused with pET28a expression vector and transferred into *E. coli* BL21 (DE3). To generate the *frr-lux* reporter fusion, the amplification products of *frr* promoter region was digested and cloned into the Xho I–BamH I site of the plasmid pMS402, which carries a promoterless *luxCDABE* reporter gene cluster. For ChIP DNA purification, *arcA* was tagged with 3×Flag, and fused with pTRC99A and electroporated into *C. sakazakii* ATCC 29544. All the strains constructed in the study were verified by sequencing. Bacteria were inoculated into fresh Luria-Bertani (LB) or M9 minimal medium (1×M9 salts, 2 mM $MgSO_4$, 0.1 mM $CaCl_2$, 0.4% glucose) and grown at 37 ºC under aerobic (250 rpm) or anaerobic (90 % N_2, 5 % CO_2, 5 % H_2; Sheldon Manufacturing) conditions. When needed, isopropyl β-D-thiogalactoside (IPTG) and antibiotics were added to the medium

at the following final concentrations: 0.1 mM IPTG, 50 μg/ml nalidixic acid, 25 μg/ml chloramphenicol (Cm), 50 μg/ml kanamycin (Kan), and 10 μg/ml tetracycline (TE).

Northern blot analysis

Total RNA (5-10 μg) was normalized and samples were mixed with 2 × RNA loading buffer (Beyotime, China). RNA was separated on 6% acrylamide gels containing 8 M urea after heating 65 ºC for 15 min. Bands were transferred to nylon membranes and crosslinked by UV. Biotinylated oligonucleotides were used as probes and hybridizations performed in the BeyoHyb™ Quick Hybridization Solution (Beyotime, China) at 42 ºC overnight. The membranes were washed twice with low stringency wash solution at room temperature for 5 min each time, and washed once at 42 ºC for 2 min. The subsequences were subjected to the Biotin Northern Blot Kit (for Small RNA) Kit (Beyotime, China). Northern blots were visualized using Amersham Imager 600, 5S ribosomal RNA (rRNA) was used as an internal control.

Race assays

Simultaneous determination of 5′ and 3′ ends of sRNA was performed using rapid amplification of complementary DNA ends (RACE) kits (Invitrogen, USA) essentially as manufacturer's instructions. The oligonucleotides used for RACE are listed in Supplementary Table 2. In each case, the generated PCR products by specific reverse primer of correct size were directly cloned into the pEASY-T1 vector (TransGen, China). Plasmids with sRNA RACE inserts were sequenced using M13 forward and reverse oligonucleotides.

Cell culture and *C. sakazakii* infection of macrophages

Murine macrophage cell line RAW264.7 (ATCC TIB-71) was obtained from the Shanghai

Institute of Biochemistry and cultured in RPMI 1640 supplemented with 10% (v/v) FBS (Hyclone, USA) at 37 °C under a 5% CO_2 atmosphere.

RAW264.7 cells were infected with WT or the indicated mutant or complemented strains that grown to the logarithmic phase at a multiplicity of infection (MOI) of 100. The cell monolayers were incubated for 45 minutes following infection, rinsed three times in PBS, and incubated for another 1 hour in RPMI 1640 media containing gentamicin (100 μg/ml) to kill the extracellular bacteria. Then each well containing bacterial cells were rinsed three times in PBS and replenished with RPMI 1640 containing gentamicin (10 μg/ml) supplemented with 1 mM $NaNO_3$ when required and incubated at 37 ºC with 5% CO_2. From this point, the hour post-infection (hpi) was deemed as 0. At 1, 4 and 24 hpi, the infected cells were washed three times with PBS and lysed with 0.05% Triton X-100 (Solarbio, China). The intracellular bacteria were enumerated on LB agar plates for CFU analysis or collected for qRT-PCR analysis. The fold intracellular replication of the indicated strains was expressed as the CFUs recovered at 4 or 24 hpi relative to those at 1 hpi.

RNA isolation and Quantitative RT–PCR (qRT–PCR)

Overnight culture of *C. sakazakii* WT strain and mutant strains were 1:100 subcultured in 20 ml fresh LB medium at 37 ºC with shaking at 180 rpm until the exponential growth phase was reached (OD_{600} = 0.6-0.8). For *C. sakazakii* collected from the cells, RAW264.7 cells were infected by *C. sakazakii* WT or mutant strains at a MOI of 100:1 and collected at 1, 4 and 24 hpi. For *C. sakazakii* collected from the small intestine and colon, 2- to 5-day-old Sprague-Dawley rat pups were orally infected by 1×10^8 CFU of *C. sakazakii* WT or mutant strains, and collected

following the contents were removed at 48 hpi. For *C. sakazakii* treated with rifampicin, *C. sakazakii* WT strain and mutant strains were incubated with 100 μg/ml of rifampicin and collected at 0, 2, 4, 8, 16, 32 min. For the effect of oxygen levels on *C. sakazakii*, mid-logarithmic phase *C. sakazakii* WT or mutant strains incubated in LB medium were collected and reincubated in M9 minimal medium supplemented under both aerobic and anaerobic conditions for 30 minutes.

Total RNA was extracted and purified using TRIzol reagent (Invitrogen, USA). RNA was treated with DNase I at 37℃ for 30 min and successful removal of DNA contamination was verified by PCR. Then the RNA was quantified and qualified by measuring the A_{260}/A_{280} absorbance ratio using a NanoDrop spectrophotometer (Thermo Fisher, USA).

cDNA synthesis was performed by StarScript III RT MasterMix (GenStar, China). qRT-PCR was performed using 2×RealStar Power SYBR qPCR Mix (Low ROX) (GenStar, China) on QuantStudio 5 (Applied Biosystems, USA). The expression levels of *C. sakazakii* transcripts were normalized to that of the *rpoA* gene [59], whereas those of the small intestine and colon transcripts were normalized to *GAPDH* expression. The fold change in the expression of each target gene was estimated using the $2^{-\Delta\Delta Ct}$ method.

RNA sequencing

Overnight-cultured bacteria of *C. sakazakii* WT and ΔCsrN strains were inoculated into fresh LB medium with a ratio of 1:100 further cultured till the OD_{600} value reached approximately 0.6, and then collected by centrifugation for RNA extraction with three biological replicates per sample. The RNA quality was assessed with an Agilent 2100 Bioanalyzer (Santa Clara, CA) and agarose

gel electrophoresis (AGE). Illumina library preparation, sequencing, and data analysis were conducted by Novogene (Bejing, China). Sequenced reads were checked for base quality, trimmed where 50% of the bases were below quality score 20, and filtered to exclude adapters. The clean reads were mapped to the *C. sakazakii* strain ATCC 29544 reference genome (CP011047.1) by using the short-sequence alignment software Bowtie 2. Gene expression levels were normalized and reported as FPKM. For differentially expressed genes (DEGs) analysis, raw read counts were normalized by TMM method and DEGs was performed using the edgeR package with a significance threshold of |log2(fold change)| > 1 and false discovery rate (FDR)-adjusted p-values < 0.005 (Benjamini-Hochberg correction).

Growth assays

For aerobic growth, overnight cultures were diluted 1:1,000 into fresh LB, RPMI 1640 medium or M9 minimal medium. Where indicated, the media were supplemented with 40 mM nitrate, 0.5 mM tungstate, or 1 mM molybdate. 200 µl aliquot was added to a 96 well microplate and incubated at 37 °C at 180 rpm for 24 h aerobically. The optical density at 600 nm was measured every 20 min. The experiment was performed in triplicate for each strain. For anaerobic growth, cultures under exponential growth phase (OD_{600} = 0.6) at a final concentration of 1×10^8 CFU/ml, supplemented as follows: (1) 40 mM $NaNO_3$; (2) 0.5 mM tungstate; (3) 1 mM molybdate; (4) 40 mM $NaNO_3$ and 0.5 mM tungstate; and (5) 40 mM $NaNO_3$ with both tungstate and molybdate at the following molar ratios, 1:2, 10:1, and 100:1, and incubated under anaerobic (90 % N_2, 5 % CO_2, 5 % H_2; Sheldon Manufacturing) [60] growth conditions at 37 ºC. The bacteria suspension was diluted with PBS and spread on agar plates for enumeration of bacterial CFUs at

1, 4 and 24 hours, respectively.

Protein expression, purification and electrophoretic mobility shift assays (EMSAs)

The constructed pET28a-ArcA plasmid was transformed into *E. coli* BL21 (DE3). pET-ArcA-containing strain was cultured overnight in LB and 1:100 subcultured in fresh LB to OD_{600} = 0.6-0.8 at 37 °C. Then IPTG was added to induce the expression of ArcA and growth at 16 °C for 20 h. The bacteria were lysed by using sonication and centrifuged at 4 °C (12,000 × g, 30 min). The supernatant containing ArcA was subsequently purified using HiTrap Ni^{2+}-chelating column. Protein concentration was determined according to the Bradford method [61].

CsrN fragments of the promotor regions and point mutant were amplified by PCR and purified using StarPrep DNA Gel Extraction Kit (GenStar, China), as well as the DNA fragments of *kana* DNA (negative control). The DNA fragment (40 ng) was incubated at 37 °C for 40 min with different concentrations of 6 × His-tagged ArcA protein (0-1.75 μM) in 20 μl binding buffer (100 mM Tris-HCl [pH 7.4], 100 mM KCl, 10mM MgCl, 10% glycerol, and 2 mM dithiothreitol). When needed, 30 mM acetyl phosphate was added to the binding system. Samples were then separated on 6% polyacrylamide gel in 0.5 × Tris-Borate-EDTA (TBE) for electrophoresis. DNA fragments were stained with GelRed (Life-iLab, China).

mRNA stability assay

Overnight culture of *C. sakazakii* WT strain and mutant strains were 1:100 subcultured in 20 ml fresh LB medium at 37 ºC with shaking at 180 rpm until the exponential growth phase was reached (OD_{600} = 0.6). The medium was then centrifuged and the bacteria were re-suspended with M9, to which rifampicin (100 μg/ml) was added. At each indicated time point after

rifampicin treatment, the same volume of bacteria was collected, and the corresponding RNA was extracted immediately for qRT-PCR.

REMSAs

The target DNA templates were transcribed into CsrN, CsrN+ (positive control), CsrN^{mut} sRNA, 5′ UTR-*narGHJI*, 5′ UTR-*narGHJI*^{mut} mRNA using T7 High Efficiency Transcription Kit (TransGen, China) and purified by MagicPure® RNA Beads (TransGen, China). REMSA was performed with CsrN, CsrN^{mut} sRNA (0, 10, 20 and 30 μM) and 5′ UTR-*narGHJI*, 5′ UTR-*narGHJI*^{mut} mRNA or CsrN+ (10 μM) in REMSA binding buffer (10 mM HEPES [pH 7.3], 20 mM KCl, 2.4 mM $MgCl_2$, and 2.4 mM DTT). The reaction mixtures were incubated for 3 min at 85 ºC and then at 37 ºC for 45 min. RNA was separated by 6% native polyacrylamide gel electrophoresis (PAGE) using a Native-PAGE Preparation kit (Sangon, China) and stained with GelRed (Life-iLab, China) for 10 min, and imaged using a gel imaging system (Tanon).

DNA affinity pull-down assay

DNA pull-down assays were conducted as previously described [62], with modifications to optimize protein-DNA interaction capture. A biotin-labeled DNA fragment encompassing the CsrN promoter region was PCR-amplified from *C. sakazakii* and immobilized on streptavidin-coated Dynabeads (Invitrogen, USA). The DNA-bound beads were incubated with crude protein extracts from *C. sakazakii* wild-type strains under optimized binding conditions. Following rigorous washing to remove nonspecifically bound proteins, the retained proteins were eluted using a high-salt buffer (500 mM NaCl), resolved by SDS-PAGE, and visualized through Coomassie Brilliant Blue staining. Protein bands of interest were excised from the gel, subjected

to in-gel tryptic digestion, and analyzed by matrix-assisted laser desorption ionization-time-of-flight tandem mass spectrometry (MALDI-TOF-MS/MS). Peptide sequences and mass spectra were compared against the NCBI non-redundant database for protein identification.

Animal model

2- to 5-day-old Sprague-Dawley rats were purchased from Beijing Vital River Laboratory Animal Technology Co., Ltd. (licensed by Charles River), and housed in specific-pathogen-free (SPF) mouse facilities. For colonization experiments, rats were infected orally with 10^8 CFU of *C. sakazakii* WT strain and mutant strains in the logarithmic phase of growth [63]. 48 hours later, blood specimens were collected for bacterial cultures (CFU). Small intestine and colon were collected and the contents were removed. Liver, spleen small intestine and colon were weighed and homogenized with PBS, and spread on agar plates for enumeration of bacterial CFUs. For survival assays, 2- to 5-day-old Sprague-Dawley rat pups were infected orally with 10^7 CFU of *C. sakazakii* WT strain and mutant strains in the logarithmic phase of growth [64]. The numbers of animals alive was recorded every 8 hours.

***In vivo* bioluminescence imaging (BLI)**

The DNA fragment of *frr* promotor were amplified, purified, and digested with BamH I/Xho I. The products were ligated to pMS402 plasmid to construct of *lux* fusion plasmids [23], which was introduced into *C. sakazakii* WT, ΔCsrN, Δ*narGHJI* and ΔCsrNΔ*narGHJI* strains, respectively. The plasmids and insertions were verified by Sanger sequencing. 2- to 5-day-old Sprague-Dawley rats were infected by oral gavage with the strains harboring *lux* fusions (10^8 CFU). At 48 hours, rats were imaged and followed by *in vivo* BLI using the *in vivo* imaging system Lumina II

(Caliper Life Sciences, USA). Data acquisition and analysis were performed using living image software (Caliper Life Sciences, USA).

Lux reporter assay

For *lux* reporter fusion, the 5′ UTR or 5′ UTR^{mut} of *narGHJI* were cloned into the pMS402 plasmid through BamH I/Xho I, respectively. For sRNA overexpression plasmids, the DNA fragments of CsrN and CsrN^{mut} were cloned into the pNM12 plasmid through Msc I/EcoR I, respectively. The empty pNM12 vector was labeled as control. The *lux* reporters and sRNA overexpression plasmids were then transformed into ΔCsrN strain. The plasmids and insertions were verified by Sanger sequencing. The expression of *lux*-based reporters from ΔCsrN strains growing in liquid culture with 0.1% arabinose (inducing the expression of sRNA) was measured using the Spark multimode microplate reader (Tecan, Switzerland).

Measurement of nitrate and nitrite concentration

The small intestine and colon of normal rat pups or that infected with *C. sakazakii* WT were collected, removed the contents and homogenized in PBS containing protease inhibitors of choice, then centrifuge at 10,000 × g for 20 minutes at 4 ºC. Transfer the supernatant to another tube as tissue samples. The cell supernatant of RAW264.7 infected with *C. sakazakii* WT at 1, 4 and 24 hpi, respectively, and uninfected cell supernatant were collected as cell samples. The following procedures were carried out according to the specification of Nitrate/Nitrite Colorimetric Assay Kit (Cayman, USA). Firstly, to determination concentration of total nitrate and nitrite, 80 μl samples were added to 96-wells, then 10 μl nitrate reductase cofactors preparation and 10 μl nitrate reductase enzyme preparation was added. After incubation for 2-3

hours, 50 µl of Griess reagent 1 and Griess reagent 2 was added, and absorbance was measured at 540nm about 10 minutes later. Secondly, to determination concentration of nitrite, 100 µl samples were added to 96-wells, then 50 µl of Griess reagent 1 and Griess reagent 2 was added, and absorbance was measured at 540nm about 10 minutes later. The nitrate concentration is equal to the total nitrate and nitrite concentration calculated using the nitrate standard curve minus the nitrite concentration calculated using the nitrite standard curve.

Cytotoxicity Assay

A lactate dehydrogenase (LDH) release assay was performed to assess cytotoxicity during bacterial infection. Following the infection of RAW264.7 cells with *C. sakazakii* WT, the indicated mutant or complemented strain, culture supernatants were collected at 1, 4 and 24 hpi. The supernatants from uninfected cells were used as a negative control. Cytotoxicity was quantified using the Cytotox 96 non-radioactive cytotoxicity assay (Promega), and the percentage of cytotoxicity was calculated according to the manufacturer's instructions.

16S rRNA gene sequencing and analysis

Caecal content samples were collected from 2- to 5-day-old rat pups, which were allocated into an untreated control group (Mock) and a tungstate-treated group (Tungstate; 48 hours of treatment), with 8 animals per group, and extracted the total DNA. The V3-V4 hypervariable region of the bacterial 16S rRNA gene was amplified by PCR using the primer pair 338F (5'-ACTCCTACGGGAGGCAGCA-3') and 806R (5'-GGACTACHVGGGTWTCTAAT-3'). The resulting PCR products were purified, and sequencing libraries were constructed. Paired-end sequencing was subsequently performed on a NextSeq 2000 system (Illumina, USA). All the

analysis was carried out on the Majorbio platform on the website at https://cloud.majorbio.com. α-diversity were calculated by software of Mothur (http://www.mothur.org/wiki/Calculators, version v1.30.2), and Principal Co-ordinates Analysis (PCoA) were conducted for the analysis of β-diversity. The comparisons among the microbiota compositions on the genus level were conducted using Vegan v2.5-3 package.

Statistics

For each experiment, the number of independent replicates is indicated in the figure legends, along with the corresponding statistical test used. Statistical significance was analyzed with GraphPad Prism 9.5.0 software (GraphPad Inc). Data were analyzed with either a Student's *t*-test to compare two conditions with normal distributions or a Mann–Whitney *U*-test for two conditions without normal distributions. For assessing statistical significance among three or more groups, a one-way analysis of variance (ANOVA), two-way ANOVA or Dunnett's test were utilized as indicated. Survival analysis was used log-rank (Mantel-Cox) test. Differences were considered significant at $p < 0.05$.

Data availability statement

RNA-seq data have been deposited in the NCBI SRA database under accession code PRJNA1278892. The proteomics data were submitted to the iProX (integrated proteome resources) (project ID: IPX0012657000). The raw sequencing data of 16S rRNA have been deposited in the Genome Sequence Archive in BIG Data Center, Beijing Institute of Genomics (BIG), Chinese Academy of Sciences, under the accession number: CRA033865. Source data are provided with this paper.

References

1 Ling, N. *et al.* Prevalence and molecular and antimicrobial characteristics of *Cronobacter* spp. isolated from raw vegetables in China. *Front Microbiol* **9**, 1149 (2018).

2 Phair, K., Pereira, S. G., Kealey, C., Fanning, S. & Brady, D. B. Insights into the mechanisms of *Cronobacter sakazakii* virulence. *Microb. Pathogen* **169**, 105643 (2022).

3 Mullane NR, I. C., Healy B, Walsh C, Whyte P, Wall PG, Quinn T, and Fanning S. *Enterobacter sakazakii* an emerging bacterial pathogen with implications for infant health. *Minerva Pediatr*, **59**, 137-148 (2007).

4 Townsend, S., Hurrell, E. & Forsythe, S. Virulence studies of *Enterobacter sakazakii* isolates associated with a neonatal intensive care unit outbreak. *BMC microbiol.* **8**, 64 (2008).

5 Friedemann, M. Epidemiology of invasive neonatal *Cronobacter* (*Enterobacter sakazakii*) infections. *Eur. J. Clin. Microbiol. Infect* **28**, 1297-1304 (2009).

6 Chauhan, R., Singh, N., Pal, G. K. & Goel, G. Trending biocontrol strategies against *Cronobacter sakazakii*: A recent updated review. *Food Res. Int.* **137**, 109385 (2020).

7 Feeney, A., Kropp, K. A., O'Connor, R. & Sleator, R. D. *Cronobacter sakazakii*: stress survival and virulence potential in an opportunistic foodborne pathogen. *Gut Microbes* **5**, 711-718 (2014).

8 Burgess, C. M. *et al.* The response of foodborne pathogens to osmotic and desiccation stresses in the food chain. *Int. J. Food Microbiol.* **221**, 37-53 (2016).

9 Pakbin, B., Brück, W. M., Allahyari, S., Rossen, J. W. & Mahmoudi, R. Antibiotic resistance and molecular characterization of *Cronobacter sakazakii* strains isolated from powdered infant formula milk. *Foods* **11**, 1093 (2022).

10 Almajed, F. S. & Forsythe, S. J. *Cronobacter sakazakii* clinical isolates overcome host barriers and evade the immune response. *Microb. Pathogen* **90**, 55-63 (2016).

11 Townsend, S. M. *et al. Enterobacter sakazakii* invades brain capillary endothelial cells, persists in human macrophages influencing cytokine secretion and induces severe brain pathology in the neonatal rat. *Microbiol.* **153**, 3538-3547 (2007).

12 Hong, S. *et al.* Crystal structures of YeiE from *Cronobacter sakazakii* and the role of sulfite tolerance in gram-negative bacteria. *Proc. Natl Acad. Sci. USA* **119**, e2118002119 (2022).

13 Bowen, A. B. & Braden, C. R. Invasive *Enterobacter sakazakii* disease in infants. *Emerg. Infect. Dis.* **12**, 1185 (2006).

14 Lee, J.-Y., Tsolis, R. M. & Bäumler, A. J. The microbiome and gut homeostasis. *Science.* **377**, eabp9960 (2022).

15 Rivera-Chávez, F. *et al.* Depletion of butyrate-producing Clostridia from the gut microbiota drives an aerobic luminal expansion of *Salmonella*. *Cell Host Microbe* **19**, 443-454 (2016).

16 Winter, S. E. *et al.* Host-derived nitrate boosts growth of *E. coli* in the inflamed gut. *Science.* **339**, 708-711 (2013).

17 Dutta, T. & Srivastava, S. Small RNA-mediated regulation in bacteria: a growing palette of diverse mechanisms. *Gene* **656**, 60-72 (2018).

18 Storz, G., Vogel, J. & Wassarman, K. M. Regulation by small RNAs in bacteria: expanding frontiers. *Mol. Cell* **43**, 880-891 (2011).

19 Sauder, A. B. & Kendall, M. M. A pathogen-specific sRNA influences enterohemorrhagic *Escherichia coli* fitness and virulence in part by direct interaction with the transcript encoding the ethanolamine utilization regulatory factor EutR. *Nucleic Acids Res.* **49**, 10988-11004 (2021).

20 Wang, M. *et al.* Genomics and experimental analysis reveal a novel factor contributing to the virulence of *Cronobacter sakazakii* strains associated with neonate infection. *J. Infect. Dis* **220**, 306-315 (2019).

21 Denman, R. B. Using RNAFOLD to predict the activity of small catalytic RNAs. *BioTechniques* **15**, 1090-1095 (1993).

22 Vogel, J. & Luisi, B. F. Hfq and its constellation of RNA. *Nat. Rev. Microbiol.* **9**, 578-589 (2011).

23 Howe, K. *et al.* Development of stable reporter system cloning *luxCDABE* genes into chromosome of *Salmonella enterica* serotypes using Tn7 transposon. *BMC Microbiol.* **10**, 197 (2010).

24 Richardson, D., Berks, B., Russell, D., Spiro, S. & Taylor, C. Functional, biochemical and genetic diversity of prokaryotic nitrate reductases. *Cell. Mol. Life Sci.* **58**, 165-178 (2001).

25 Mann, M., Wright, P. R. & Backofen, R. IntaRNA 2.0: enhanced and customizable prediction of RNA–RNA interactions. *Nucleic Acids Res.* **45**, W435-W439 (2017).

26 Gillis, C. C. *et al.* Dysbiosis-associated change in host metabolism generates lactate to support *Salmonella*

growth. *Cell Host Microbe* **23**, 54-64. e56 (2018).

27 Lundberg, J. O., Weitzberg, E. & Gladwin, M. T. The nitrate–nitrite–nitric oxide pathway in physiology and therapeutics. *Nat. Rev. Drug Discov.* **7**, 156-167 (2008).

28 Wu, K. K.-l. *et al.* MDM2 induces pro-inflammatory and glycolytic responses in M1 macrophages by integrating iNOS-nitric oxide and HIF-1α pathways in mice. *Nat. Commun.* **15**, 8624 (2024).

29 Fukuda, M. *et al.* Structural basis for dynamic mechanism of nitrate/nitrite antiport by NarK. *Nat. Commun.* **6**, 7097 (2015).

30 Bueno, E., Sit, B., Waldor, M. & Cava, F. Anaerobic nitrate reduction divergently governs population expansion of the enteropathogen *Vibrio cholerae*. *Nat. Microbiol.* **3**, 1346–1353 (2018).

31 Zhou, Y. *et al.* Thiol-based functional mimicry of phosphorylation of the two-component system response regulator ArcA promotes pathogenesis in enteric pathogens. *Cell Rep.* **37** (2021).

32 Compan, I. & Touati, D. Anaerobic activation of arcA transcription in *Escherichia coli*: roles of Fnr and ArcA. *Mol. Microbiol.* **11**, 955-964 (1994).

33 Cunningham-Bussel, A., Zhang, T. & Nathan, C. F. Nitrite produced by Mycobacterium tuberculosis in human macrophages in physiologic oxygen impacts bacterial ATP consumption and gene expression. *Proc. Natl Acad. Sci. USA* **110**, E4256-E4265 (2013).

34 Kuo, C.-J. *et al.* A multi-omic analysis reveals the role of fumarate in regulating the virulence of enterohemorrhagic *Escherichia coli*. *Cell Death Dis.* **9**, 381 (2018).

35 Qin, Y. *et al.* Colonic mucus-accumulating tungsten oxide nanoparticles improve the colitis therapy by targeting *Enterobacteriaceae*. *Nano Today* **39**, 101234 (2021).

36 Zhu, L. *et al.* Arachidonic acid metabolism regulates *Escherichia coli* penetration of the blood-brain barrier. *Infect. Immun.* **78**, 4302-4310 (2010).

37 Unden, G., Strecker, A., Kleefeld, A. & Kim, O. B. C4-dicarboxylate utilization in aerobic and anaerobic growth. *EcoSal Plus* **7**, 10.1128/ecosalplus. ESP-0021-2015 (2016).

38 Weitzberg, E., Hezel, M., Lundberg, J. O. & Warner, D. S. Nitrate-nitrite-nitric oxide pathway: implications for anesthesiology and intensive care. *Anesthesiology* **113**, 1460-1475 (2010).

39 Zheng, L., Kelly, C. J. & Colgan, S. P. Physiologic hypoxia and oxygen homeostasis in the healthy intestine.

A review in the theme: cellular responses to hypoxia. *Am J Physiol Cell Physiol.* **309**, C350-C360 (2015).

40 Richardson, A. R., Libby, S. J. & Fang, F. C. A nitric oxide–inducible lactate dehydrogenase enables *Staphylococcus aureus* to resist innate immunity. *Science* **319**, 1672-1676 (2008).

41 Nathan, C. & Shiloh, M. U. Reactive oxygen and nitrogen intermediates in the relationship between mammalian hosts and microbial pathogens. *Proc. Natl Acad. Sci. USA* **97**, 8841-8848 (2000).

42 Kandhai, M. C., Reij, M. W., Gorris, L. G., Guillaume-Gentil, O. & van Schothorst, M. Occurrence of *Enterobacter sakazakii* in food production environments and households. *Lancet* **363**, 39-40 (2004).

43 Healy, B. *et al. Cronobacter* (*Enterobacter sakazakii*): an opportunistic foodborne pathogen. *Foodborne Pathog. Dis.* **7**, 339-350 (2010).

44 Bowden, S. D., Ramachandran, V. K., Knudsen, G. M., Hinton, J. C. & Thompson, A. An incomplete TCA cycle increases survival of *Salmonella Typhimurium* during infection of resting and activated murine macrophages. *PloS one* **5**, e13871 (2010).

45 Alteri, C. J., Smith, S. N. & Mobley, H. L. Fitness of *Escherichia coli* during urinary tract infection requires gluconeogenesis and the TCA cycle. *PLoS Pathog.* **5**, e1000448 (2009).

46 Lencina, A. M. *et al.* Type 2 NADH dehydrogenase is the only point of entry for electrons into the *Streptococcus agalactiae* respiratory chain and is a potential drug target. *mBio* **9**, 10.1128/mbio. 01034-01018 (2018).

47 Koganitsky, A., Tworowski, D., Dadosh, T., Cecchini, G. & Eisenbach, M. A mechanism of modulating the direction of flagellar rotation in bacteria by fumarate and fumarate reductase. *J. Mol. Biol.* **431**, 3662-3676 (2019).

48 Ferraro, C. M. & Finkel, S. E. Physiological, genetic, and transcriptomic analysis of alcohol-induced delay of *Escherichia coli* death. *Appl Environ Microbiol.* **85**, e02113-02118 (2019).

49 McCrindle, S. L., Kappler, U. & McEwan, A. G. Microbial dimethylsulfoxide and trimethylamine-N-oxide respiration. *Adv. Microb. Physiol.* **50**, 147-201e (2005).

50 Haston, J. C. *Cronobacter sakazakii* infections in two infants linked to powdered infant formula and breast pump equipment—United States, 2021 and 2022. *Morb Mortal Wkly Rep.* **72** (2023).

51 Fei, P. *et al.* Antibiotic and desiccation resistance of *Cronobacter sakazakii* and *C. malonaticus* isolates from

powdered infant formula and processing environments. *Front. Microbiol.* **8**, 316 (2017).

52 Li, Y. *et al.* Prevalence and genetic characteristics of *Cronobacter* spp. from food and human clinical stool samples in Wenzhou, China 2008–2018. *Food Microbiol.* **89**, 103432 (2020).

53 Carvalho, G. G. *et al.* Isolation, comparison of identification methods and antibiotic resistance of *Cronobacter* spp. in infant foods. *Food Res. Int.* **137**, 109643 (2020).

54 Parra-Flores, J. *et al.* Virulence and antibiotic resistance profiles of *Cronobacter sakazakii* and *Enterobacter* spp. involved in the diarrheic hemorrhagic outbreak in Mexico. *Front. Microbiol.* **9**, 2206 (2018).

55 Fishbein, S. R., Mahmud, B. & Dantas, G. Antibiotic perturbations to the gut microbiome. *Nat. Rev. Microbiol.* **21**, 772-788 (2023).

56 Akagawa, S. *et al.* Development of the gut microbiota and dysbiosis in children. *Biosci. Microbiota Food Health.* **40**, 12-18 (2021).

57 Zhu, W. *et al.* Precision editing of the gut microbiota ameliorates colitis. *Nature.* **553**, 208-211 (2018).

58 Datsenko, K. A. & Wanner, B. L. One-step inactivation of chromosomal genes in *Escherichia coli* K-12 using PCR products. *Proc. Natl Acad. Sci. USA* **97**, 6640-6645 (2000).

59 Melson, E. M. & Kendall, M. M. The sRNA DicF integrates oxygen sensing to enhance enterohemorrhagic *Escherichia coli* virulence via distinctive RNA control mechanisms. *Proc. Natl Acad. Sci. USA* **116**, 14210-14215 (2019).

60 Hughes, E. R. *et al.* Microbial respiration and formate oxidation as metabolic signatures of inflammation-associated dysbiosis. *Cell Host Microbe* **21**, 208-219 (2017).

61 Mm, B. A rapid and sensitive method for the quantitation of microgram quantities of protein utilizing the principle of protein-dye binding. *Anal. Biochem.* **72**, 248-254 (1976).

62 Jutras, B. L., Verma, A. & Stevenson, B. Identification of novel DNA‐binding proteins using DNA‐affinity chromatography/pull down. *Curr. Protoc. Microbiol.* **Chapter 1**, 1 (2012).

63 Richardson, A. N., Beuchat, L. R., Lambert, S., Williams, D. & Smith, M. A. Comparison of virulence of three strains of *Cronobacter sakazakii* in neonatal CD-1 mice. *J. Food Prot.* **73**, 849-854 (2010).

64 Ji, X. *et al.* The lipoprotein NlpD in *Cronobacter sakazakii* responds to acid stress and regulates macrophage resistance and virulence by maintaining membrane integrity: running Title: identification and

characterization of a novel factor involved in acid tolerance and virulence in *Cronobacter sakazakii*. *Virulence* **12**, 415-429 (2021).

Acknowledgments

This work was supported by grants from the National Natural Science Foundation of China (82372267 to B.L., 82402643 to H.S., W2512084 to B.L., 82572591 to B.L., 32070133 to L.F., 32470111 to L.F., 32130003 to L.W., 32370194 to L.W.), grants from the Natural Science Foundation of Shenzhen Province of China (JCYJ20220530164604010 to B.L., JCYJ20230807151559009 to B.L.), a grant from Guangdong Basic and Applied Basic Research Foundation of China (2024A1515010588 to B.L.), a grant from Key Laboratory Major Project of 2024 (Tianjin) (25ZXZSSS00710 to B.L.) and a grant from Fundamental Research Funds for Central Universities of China (63233172 to B.L.).

Author contributions

Conceptualization, B.L., L.W., X.L. and H.S.; methodology, X.L., H.S., X.Y., L.F., Y.N., B.X., J.Q., J.W., Z.L., L.W. and L.F.; visualization, X.L. and H.S.; supervision, B.L.; writing–original draft, B.L., L.W., X.L. and H.S.; writing– review & editing, B.L., L.W., X.L. and H.S..

Declaration of interests

The authors declare no competing interests.

Figure legends

Figure 1. Identification and characterization of the sRNA CsrN in *C. sakazakii*. (A) The position of CsrN sequence in the genome of *C. sakazakii* ATCC 29544. **(B)** qRT-PCR analysis of *C. sakazakii* CsrN expression in RAW264.7 at 1, 4, 24 h post infection (hpi) compared with that in LB medium. n = 3 independent experiments. **(C)** Northern blot analysis of CsrN expression in *C. sakazakii* WT, ΔCsrN and ΔCsrN complemented (ΔCsrN+pCsrN) strains. 5S rRNA (ribosomal RNA) served as a loading control. n = 3 independent experiments. **(D)** Secondary structures of CsrN sRNA were predicated using RNAfold (http://rna.tbi.univie.ac.at/). In **(B)**, the data are presented as the mean ± SD. Two-tailed Student's *t* test (**B**) were applied. Source data are provided as a Source Data file.

Figure 2. CsrN enhances *C. sakazakii* virulence *in vitro* and *in vivo*. (A) Bacterial burdens of *C. sakazakii* WT, ΔCsrN or ΔCsrN+pCsrN strain in RAW264.7 at 1, 4 and 24 hpi. n = 3 independent experiments. **(B)** Bacterial counts recovered from the blood, liver, spleen, small intestine, and colon of 2- to 5-day-old rats orally infected with 1×10^8 CFU of *C. sakazakii* WT, ΔCsrN or ΔCsrN+pCsrN strain at 48 hpi. n = 8 rats per group. **(C)** Survival curves of rats orally infected with 1×10^7 CFU of the *C. sakazakii* WT, ΔCsrN or ΔCsrN+pCsrN strain. n = 12 rats per group. **(D)** *In vivo* bioluminescent imaging of rats orally infected with 1×10^8 CFU of the WT-Lux, ΔCsrN-Lux or ΔCsrN+pCsrN-Lux strain at 48 hpi. n = 6 rats per group. Box plot bounds represent the interquartile range between the 25th and 75th percentiles with the horizontal bar representing the median. Whiskers extend to the full range of data. **(E-F)** Representation images **(E)** and histological score **(F)** of rat colon orally infected with 1×10^8 CFU of *C. sakazakii* WT, ΔCsrN or ΔCsrN+pCsrN strain at 48 hpi. n = 5 rats per group. ns, nonsignificant. In (**A** and **F**), the data are presented as the mean ± SD. One-way ANOVA (**A**), Two-tailed Mann-Whitney *U* test (**B**, **D** and **F**), the log-rank (Mantel-Cox) test **(C)** were applied. Source data are provided as a Source Data file.

Figure 3. CsrN binds to the 5′ UTR of *narHJI* to enhance *narGHJI* expression by stabilizing its mRNA. (A) The volcano plot of differentially expressed genes (DEGs) in *C. sakazakii* WT and ΔCsrN strains in LB medium. **(B)** KEGG Chord plot of 10 related KEGG pathways. Chords indicated a detailed relationship between expression levels of DEGs (left semicircle perimeter) and their enriched KEGG pathways (right semicircle perimeter). **(C)** The position of *narGHJI* cluster in the genome of *C. sakazakii* ATCC 29544. **(D-F)** qRT-PCR analysis of *narGHJI* expression in the *C. sakazakii* WT and ΔCsrN strains in LB medium **(D)**, RAW264.7 at 24 hpi **(E)** or small intestine of rats infected with WT or ΔCsrN at 48 hpi **(F)**. n = 3 independent experiments. **(G)** Predicted CsrN-5′ UTR of *narGHJI* RNA base pairing. Point mutations to generate the disrupted alleles. **(H-K)** REMSA of CsrN and 5′ UTR of *narGHJI* **(H)**, $CsrN^{mut}$ and 5′ UTR of *narGHJI* **(I)**, CsrN and 5′ UTR^{mut} of *narGHJI* **(J)**, and $CsrN^{mut}$ and 5′ UTR^{mut} of *narGHJI* **(K)**. **(L-M)** Expression of the 5′ UTR or 5′ UTR^{mut} of *narGHJI-lux* fusion when CsrN or $CsrN^{mut}$ was overexpressed as indicated. n = 3 independent experiments. **(N-O)** qRT-PCR analysis of *narH* **(N)** and *narJ* **(O)** expression in rifampicin-treated *C. sakazakii* WT, ΔCsrN and ΔCsrN+pCsrN strains. n = 3 independent experiments. ns, nonsignificant. In **(D-F** and **L-O)**, the data are presented as the mean ± SD. For differentially expressed genes (DEGs) analysis, raw read counts were normalized by TMM method and DEGs was performed using the edgeR package with a significance threshold of |log2(fold change)| > 1 and false discovery rate (FDR)-adjusted p-values < 0.005 (Benjamini-Hochberg correction). **(A)**. Two-tailed Student's *t* test (**D-F**), One-way ANOVA **(L-M),** Two-way ANOVA **(N-O)** were applied. Source data are provided as a Source Data file.

Figure 4. *narGHJI* promotes the pathogenicity of *C. sakazakii.* (A) Bacterial burdens of *C. sakazakii* WT, Δ*narGHJI*, ΔCsrNΔ*narGHJI* or Δ*narGHJI* complemented (Δ*narGHJI*+p*narGHJI*) strains in RAW264.7 at 1, 4 and 24 hpi. n = 3 independent experiments. **(B)** Bacterial counts recovered from the blood, liver, spleen, small intestine, and colon of 2- to 5-day-old rats orally infected with 1×10^8 CFU of *C. sakazakii* WT, Δ*narGHJI*, ΔCsrNΔ*narGHJI* or Δ*narGHJI*+p*narGHJI* strain at 48 hpi. n = 8 rats per group. **(C)** Survival curves of rats orally infected with 1×10^7 CFU of the *C. sakazakii* WT, Δ*narGHJI*, ΔCsrNΔ*narGHJI* or Δ*narGHJI*+p*narGHJI* strain. n = 12 rats per group. **(D)** *In vivo* bioluminescent imaging of rats orally infected with 1×10^8 CFU of the WT-Lux, Δ*narGHJI*-Lux or Δ*narGHJI*+p*narGHJI*-Lux strain at 48 hpi. n = 6 rats per group. Box plot bounds represent the interquartile range between the 25th and 75th percentiles with the horizontal bar representing the median. Whiskers extend to the full range of data. **(E-F)** Representation images **(E)** and histological score **(F)** of rat colon orally infected with 1×10^8 CFU of *C. sakazakii* WT, Δ*narGHJI* or Δ*narGHJI*+p*narGHJI* at 48 hpi. n = 5 rats per group. ns, nonsignificant. In **(A** and **F)**, the data are presented as the mean ± SD. One-way ANOVA **(A)**, Two-tailed Mann-Whitney *U* test **(B, D** and **F)**, the log-rank (Mantel-Cox) test **(C)** were applied. Source data are provided as a Source Data file.

Figure 5. Nitrate respiration is essential for full virulence of *C. sakazakii*. **(A)** Nitrate levels in small intestine, and colon of 2- to 5-day-old rats orally infected with 1×10^8 CFU of *C. sakazakii* WT at 48 hpi versus those uninfected. n = 6 rats per group. **(B)** Nitrate levels in RAW264.7 uninfected or infected with *C. sakazakii* WT at 0, 1, 4 and 24 hpi. n = 3 independent experiments. **(C-D)** qRT-PCR analysis of *Nos2* and *Tnf* expression in the small intestine and colon of rats at 48 hpi **(C)** or RAW264.7 at 1, 4 and 24 hpi **(D)** infected with *C. sakazakii* WT strain versus those uninfected. n = 3 independent experiments. **(E)** qRT-PCR analysis of *narGHJI* and *narK* expression in *C. sakazakii* WT strain in RAW264.7 at 24 hpi compared with that grown in LB medium. n = 3 independent experiments. **(F)** Bacterial burdens of *C. sakazakii* WT and Δ*narK* strains in RAW264.7 at 1, 4 and 24 hpi. n = 3 independent experiments. **(G)** Bacterial counts recovered form in blood, liver, spleen, small intestine, and colon of 2- to 5-day-old rats orally infected with 1×10^8 CFU of *C. sakazakii* WT or Δ*narK* strain at 48 hpi. n = 8 rats per group. **(H)** Replication of *C. sakazakii* WT, Δ*narGHJI* and Δ*narK* strains in LB medium with or without $NaNO_3$ in anaerobic environments. Relative replication ratio was the fold change in growth at 1, 4, and 24 hours / 0 hours. n = 3 independent experiments. **(I)** Replication of *C. sakazakii* WT, Δ*narGHJI* and Δ*narK* strains in RAW264.7 with or without $NaNO_3$. Relative replication ratio was the fold change in bacterial burdens at 4 and 24 hpi / 1 hpi. n = 3 independent experiments. ns, nonsignificant. In **(A-F** and **H-I)**, the data are presented as the mean ± SD. Two-tailed Student's *t* test **(A** and **C-F)**, Two-tailed Mann-Whitney *U* test **(G)**, Two-way ANOVA **(B** and **H-I)** were applied. Source data are provided as a Source Data file.

Figure 6. ArcAB senses anaerobic condition to enhance *narGHJI* expression via CsrN. (A) qRT-PCR analysis of CsrN expression in the *C. sakazakii* WT and Δ*arcA* in LB medium. n = 3 independent experiments. **(B)** qRT-PCR analysis of CsrN and *narGHJI* expression in WT- or Δ*arcA*-infected RAW264.7 at 24 hpi. n = 3 independent experiments. **(C)** qRT-PCR analysis of *narGHJI* expression in ΔCsrN and ΔCsrNΔ*arcA* strains in LB medium. n = 3 independent experiments. **(D)** EMSA of the CsrN promoter (CsrN-pro) with purified ArcA protein. **(E)** The fold enrichment of the promoters for CsrN (P_{CsrN}) and the negative control (*rpoS*) in ArcA-chromatin immunoprecipitation (ChIP) samples. n = 3 independent experiments. **(F-I)** Northern blot analysis **(F** and **H)** and qRT-PCR analysis **(G** and **I)** of CsrN and *narGHJI* expression in the *C. sakazakii* WT **(F-G)** and Δ*arcA* **(H-I)** under aerobic and anaerobic conditions. n = 3 independent experiments. **(J)** Bacterial counts recovered form blood, liver, spleen, small intestine, and colon of 2- to 5-day-old rats orally infected with 1×10^8 CFU of *C. sakazakii* WT, Δ*arcA* or Δ*arcA*+p*arcA* strain at 48 hpi. n = 8 rats per group. ns, nonsignificant. In **(A-C** and **E-I)**, the data are presented as the mean ± SD. Two-tailed Student's *t*-test **(A-C** and **E-I)**, Two-tailed Mann-Whitney *U* test **(J)** were applied. Source data are provided as a Source Data file.

Figure 7. Nitrate respiration is a crucial energy metabolic pathway in *C. sakazakii*. (A) Replication of *C. sakazakii* WT, Δ*cydAB*, Δ*frdABCD*, Δ*dmsABC*, Δ*adhE* or Δ*ldhA* strains in LB medium under anaerobic environments. Relative replication ratio was the fold change in growth at 1, 4, and 24 hours / 0 hours. n = 3 independent experiments. **(B)** Bacterial burdens of *C. sakazakii* WT, Δ*cydAB*, Δ*frdABCD*, Δ*dmsABC*, Δ*adhE* or Δ*ldhA* strains in RAW264.7 at 1, 4 and 24 hpi. n = 3 independent experiments. **(C)** Bacterial counts recovered from the blood, liver, spleen, small intestine, and colon of 2- to 5-day-old rats orally infected with 1×10^8 CFU of *C. sakazakii* WT, Δ*cydAB*, Δ*frdABCD*, Δ*dmsABC*, Δ*adhE* or Δ*ldhA* strains at 48 hpi. n = 8 rats per group. **(D-E)** Bacterial counts recovered from the blood, liver, spleen, small intestine, and colon of tungstate-treated or untreated rats orally infected with 1×10^8 CFU of *C. sakazakii* WT strain **(D)**, or Δ*narGHJI* strain **(E)** at 48 hpi. n = 8 rats per group. ns, nonsignificant. In **(A** and **B)**, the data are presented as the mean ± SD. Two-way ANOVA **(A)**, One-way ANOVA **(B)**, Two-tailed Mann-Whitney *U* test **(C**-**E)** were applied. Source data are provided as a Source Data file.

Figure 8. CsrN-Mediated regulation of nitrate respiration enhances *C. sakazakii* survival under anaerobic conditions in the gut.

Editor's Summary

This study reveals an sRNA-centered signaling pathway which activates nitrate respiration and enhances Cronobacter sakazakii virulence in oxygen-limited host environments, offering important insights into therapeutic strategies.

Peer review information: *Nature Communications* thanks Charlotte Michaux, Haiyan Zeng and the other, anonymous, reviewer(s) for their contribution to the peer review of this work. A peer review file is available.

A

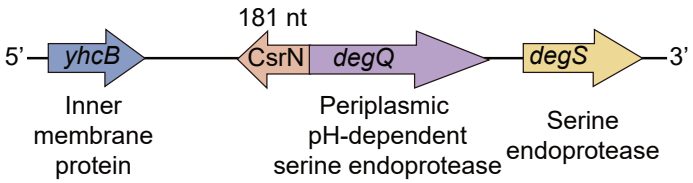

CsrN sequence

+1 (transcription start site)

5'- GCACTTAACAGCAGGGTTTGTTTTTTCATGAACGCAGC

TCTCGCAACCTGGTTATAAAAGTCACCTGAAAACACGGAT

ATTATTGAATTCTCAATGTCGTAACAATGCTGTCATCGGGA

CGGCAGCGCTCAGAATAAGCATAGTCAGCGCCCAAAGAA

AAGCGGGCGCAAATGCGCCCGAC -3'

B

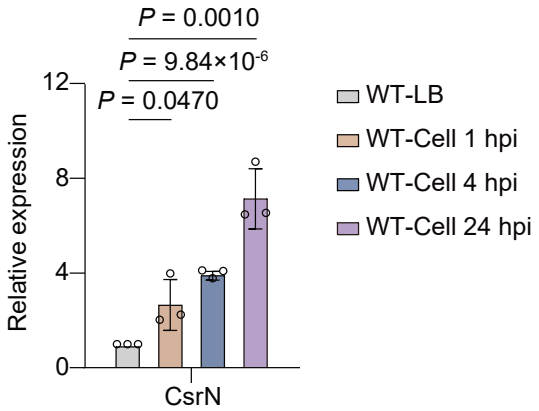

C

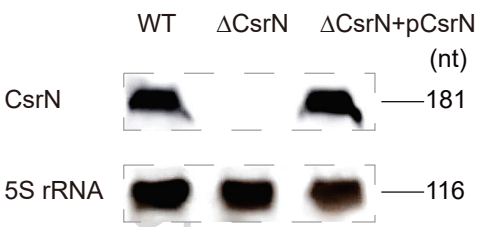

D

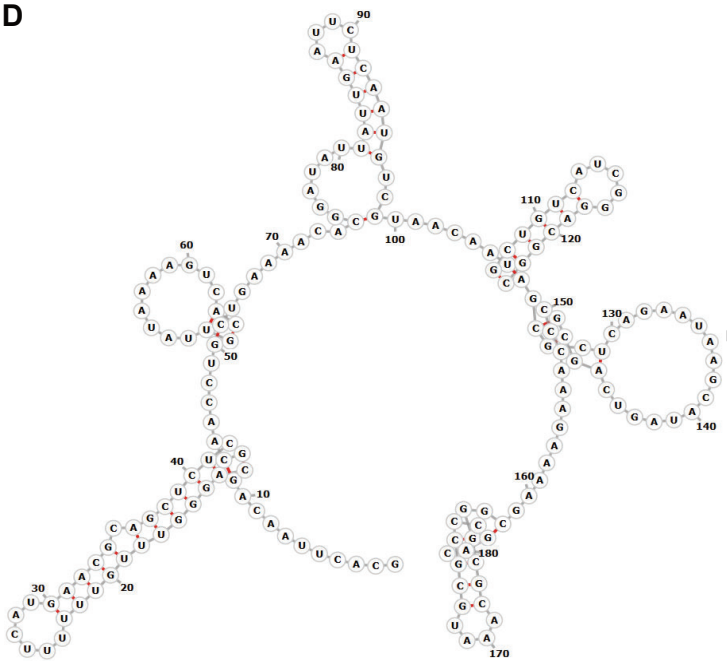

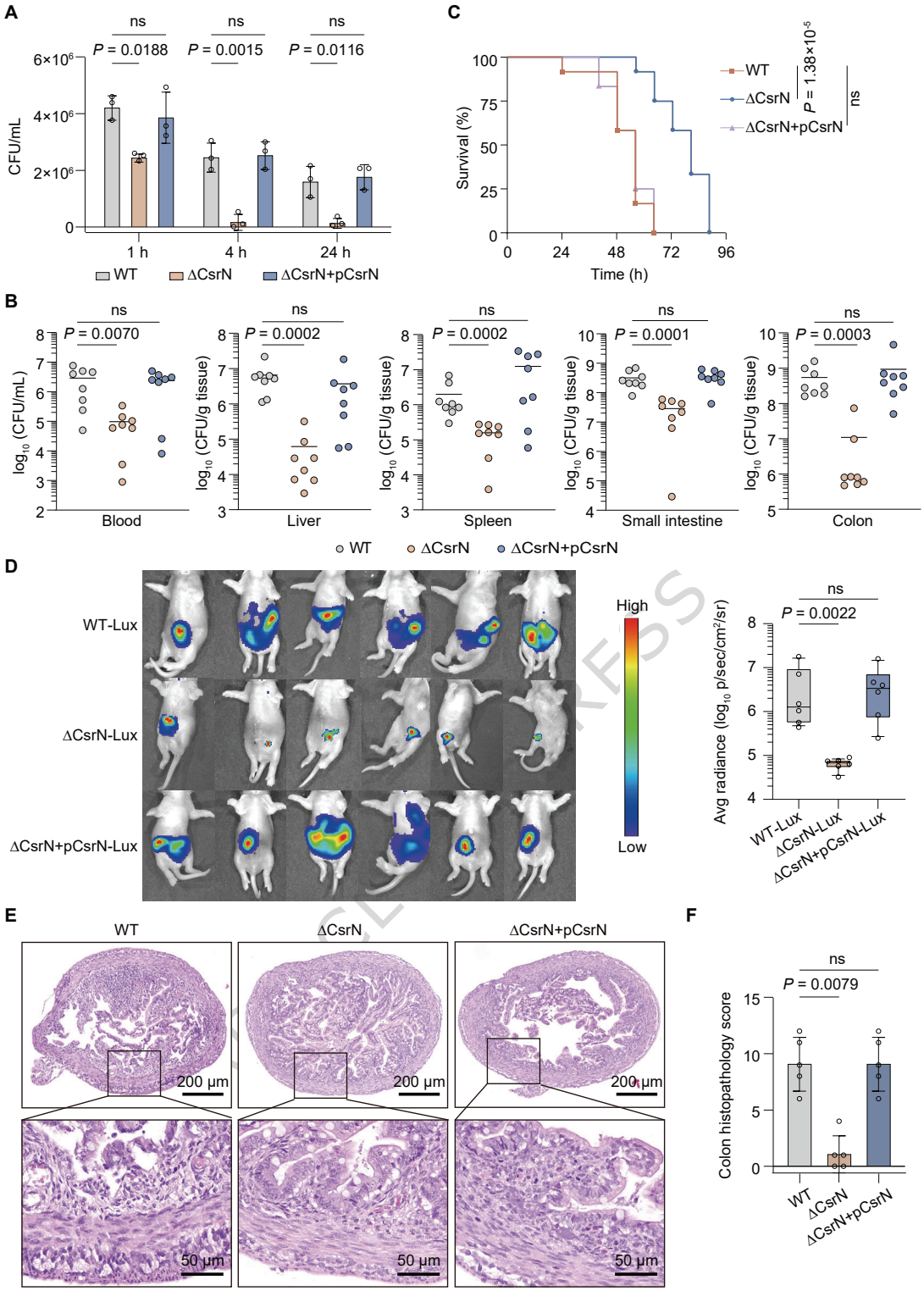
A
ns
P = 0.0188
P = 0.0015
P = 0.0116
CFU/mL
1 h
4 h
24 h
WT
ΔCsrN
ΔCsrN+pCsrN
C
Survival (%)
Time (h)
WT
ΔCsrN
ΔCsrN+pCsrN
P = 1.38×10-5
ns
B
P = 0.0070
P = 0.0002
P = 0.0002
P = 0.0001
P = 0.0003
log10 (CFU/mL)
log10 (CFU/g tissue)
Blood
Liver
Spleen
Small intestine
Colon
D
WT-Lux
ΔCsrN-Lux
ΔCsrN+pCsrN-Lux
High
Low
P = 0.0022
Avg radiance (log10 p/sec/cm2/sr)
E
WT
ΔCsrN
ΔCsrN+pCsrN
200 μm
50 μm
F
P = 0.0079
Colon histopathology score

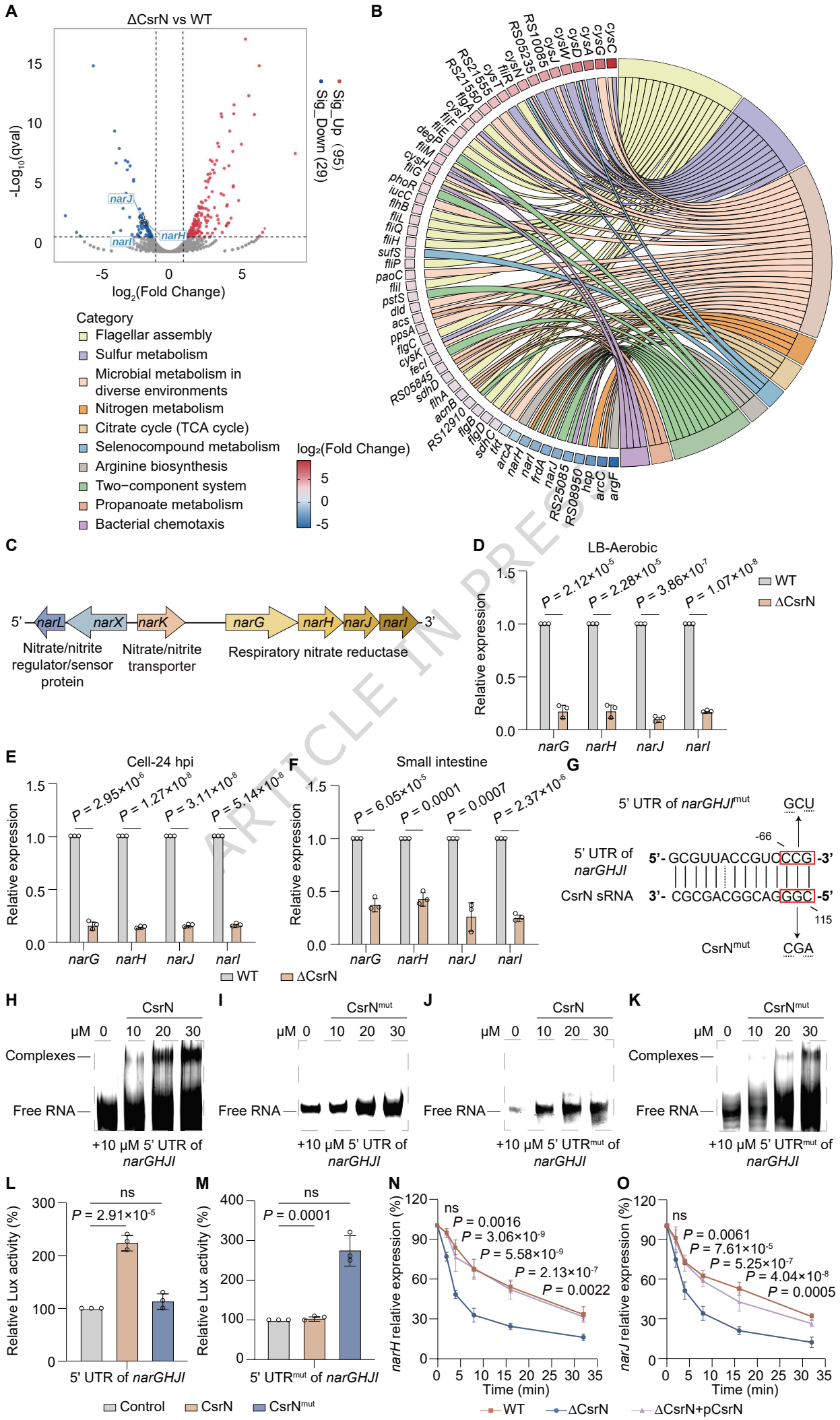
A
ΔCsrN vs WT
-Log10(qval)
log2(Fold Change)
Sig_Up (95)
Sig_Down (29)
narJ
narI
narH
Category
Flagellar assembly
Sulfur metabolism
Microbial metabolism in diverse environments
Nitrogen metabolism
Citrate cycle (TCA cycle)
Selenocompound metabolism
Arginine biosynthesis
Two−component system
Propanoate metabolism
Bacterial chemotaxis
log2(Fold Change)
B
C
narL
narX
narK
narG
narH
narJ
narI
Nitrate/nitrite regulator/sensor protein
Nitrate/nitrite transporter
Respiratory nitrate reductase
D
LB-Aerobic
Relative expression
WT
ΔCsrN
E
Cell-24 hpi
F
Small intestine
G
5' UTR of narGHJI mut
GCU
-66
5' UTR of narGHJI
5'- GCGUUACCGUCCCG -3'
CsrN sRNA
3'- CGCGACGGCAGGGC -5'
115
CsrN mut
CGA
H
CsrN
Complexes
Free RNA
+10 μM 5' UTR of narGHJI
I
CsrN mut
+10 μM 5' UTR of narGHJI
J
CsrN
+10 μM 5' UTR mut of narGHJI
K
CsrN mut
+10 μM 5' UTR mut of narGHJI
L
Relative Lux activity (%)
5' UTR of narGHJI
M
5' UTR mut of narGHJI
Control
CsrN
CsrN mut
N
narH relative expression (%)
Time (min)
WT
ΔCsrN
ΔCsrN+pCsrN
O
narJ relative expression (%)

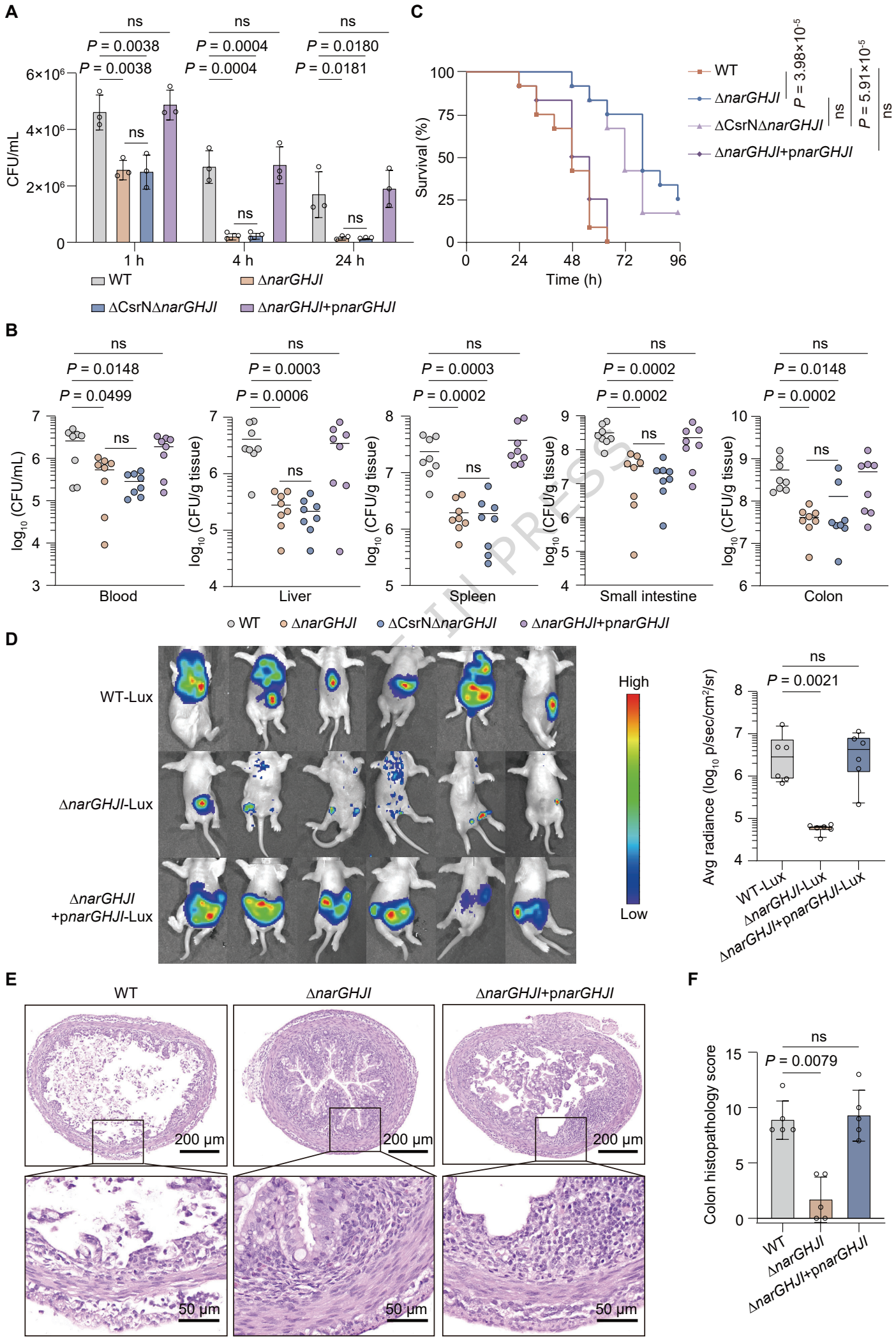
A
ns
P = 0.0038
P = 0.0038
P = 0.0004
P = 0.0004
P = 0.0180
P = 0.0181
CFU/mL
1 h
4 h
24 h
WT
ΔnarGHJI
ΔCsrNΔnarGHJI
ΔnarGHJI+pnarGHJI
C
Survival (%)
Time (h)
P = 3.98×10-5
P = 5.91×10-5
B
P = 0.0148
P = 0.0499
P = 0.0003
P = 0.0006
P = 0.0002
P = 0.0002
P = 0.0002
P = 0.0148
Blood
Liver
Spleen
Small intestine
Colon
D
WT-Lux
ΔnarGHJI-Lux
ΔnarGHJI +pnarGHJI-Lux
High
Low
P = 0.0021
Avg radiance (log10 p/sec/cm2/sr)
E
200 μm
50 μm
F
P = 0.0079
Colon histopathology score

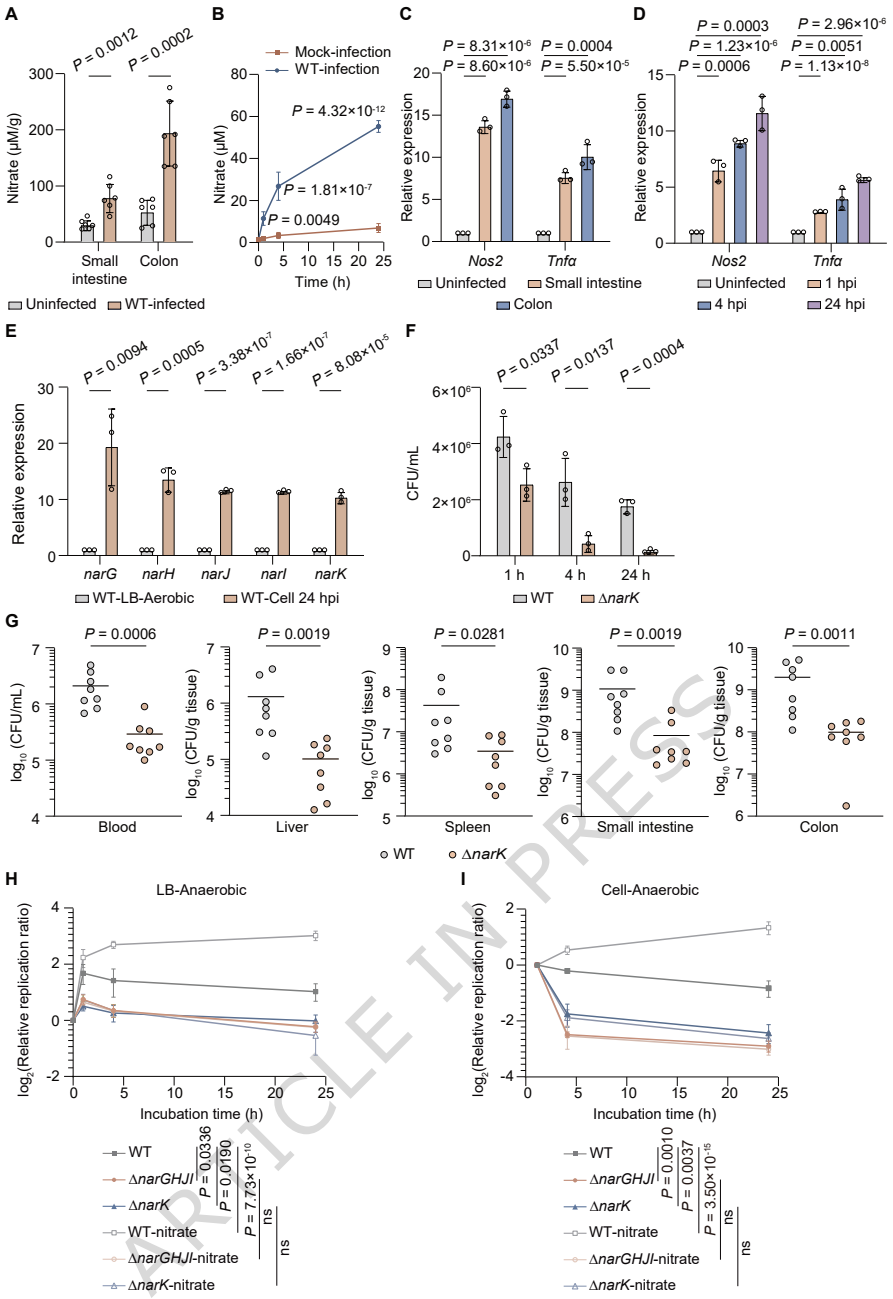

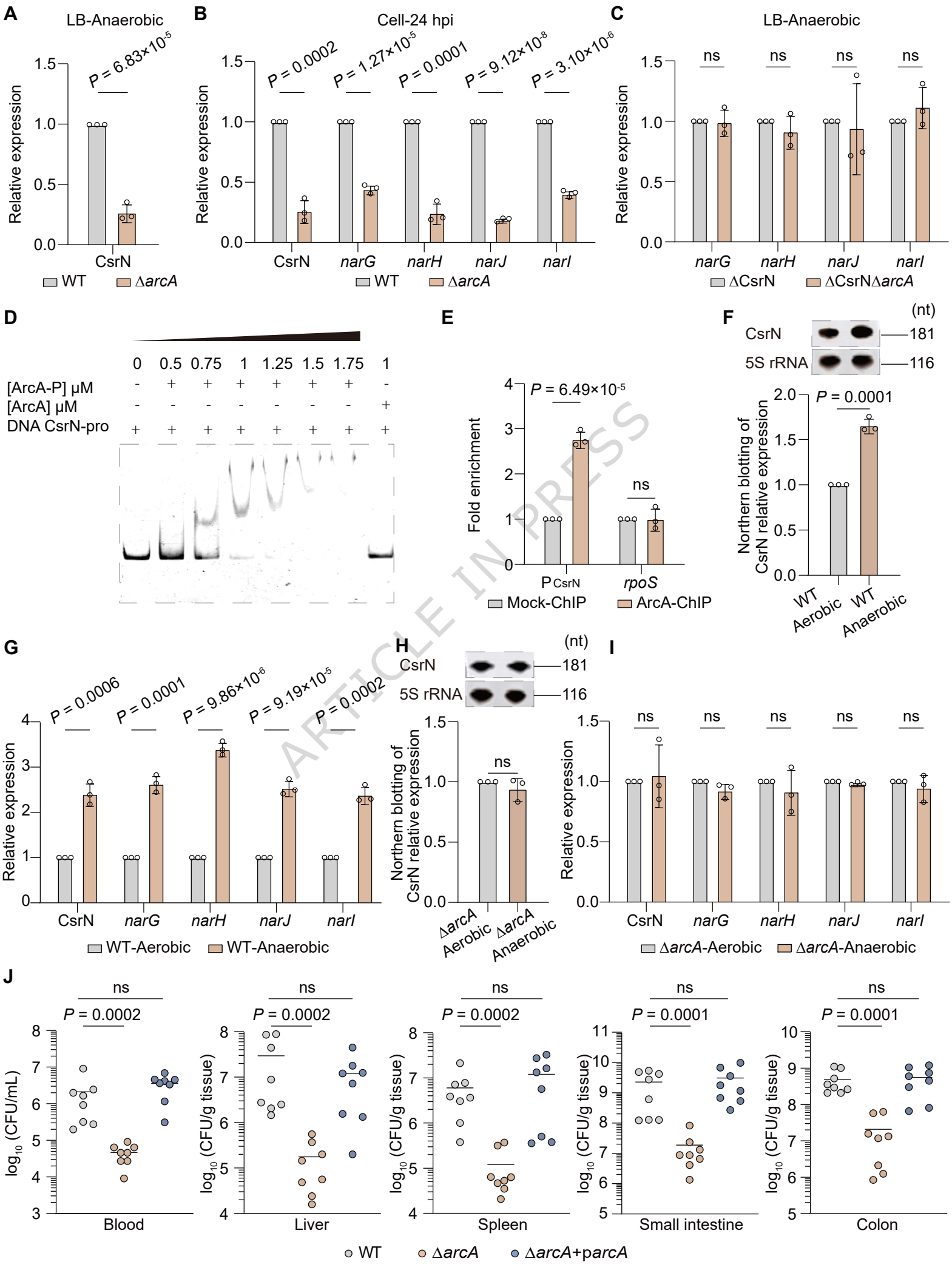
A
LB-Anaerobic
P = 6.83×10-5
Relative expression
CsrN
WT
ΔarcA
B
Cell-24 hpi
P = 0.0002
P = 1.27×10-5
P = 0.0001
P = 9.12×10-8
P = 3.10×10-6
CsrN
narG
narH
narJ
narI
C
LB-Anaerobic
ns
ΔCsrN
ΔCsrNΔarcA
D
0 0.5 0.75 1 1.25 1.5 1.75 1
[ArcA-P] μM
[ArcA] μM
DNA CsrN-pro
E
P = 6.49×10-5
Fold enrichment
PCsrN
rpoS
Mock-ChIP
ArcA-ChIP
F
(nt)
CsrN
5S rRNA
181
116
P = 0.0001
Northern blotting of CsrN relative expression
WT Aerobic
WT Anaerobic
G
P = 0.0006
P = 0.0001
P = 9.86×10-6
P = 9.19×10-5
P = 0.0002
WT-Aerobic
WT-Anaerobic
H
ΔarcA Aerobic
ΔarcA Anaerobic
I
ΔarcA-Aerobic
ΔarcA-Anaerobic
J
P = 0.0002
P = 0.0001
log10 (CFU/mL)
log10 (CFU/g tissue)
Blood
Liver
Spleen
Small intestine
Colon
WT
ΔarcA
ΔarcA+parcA

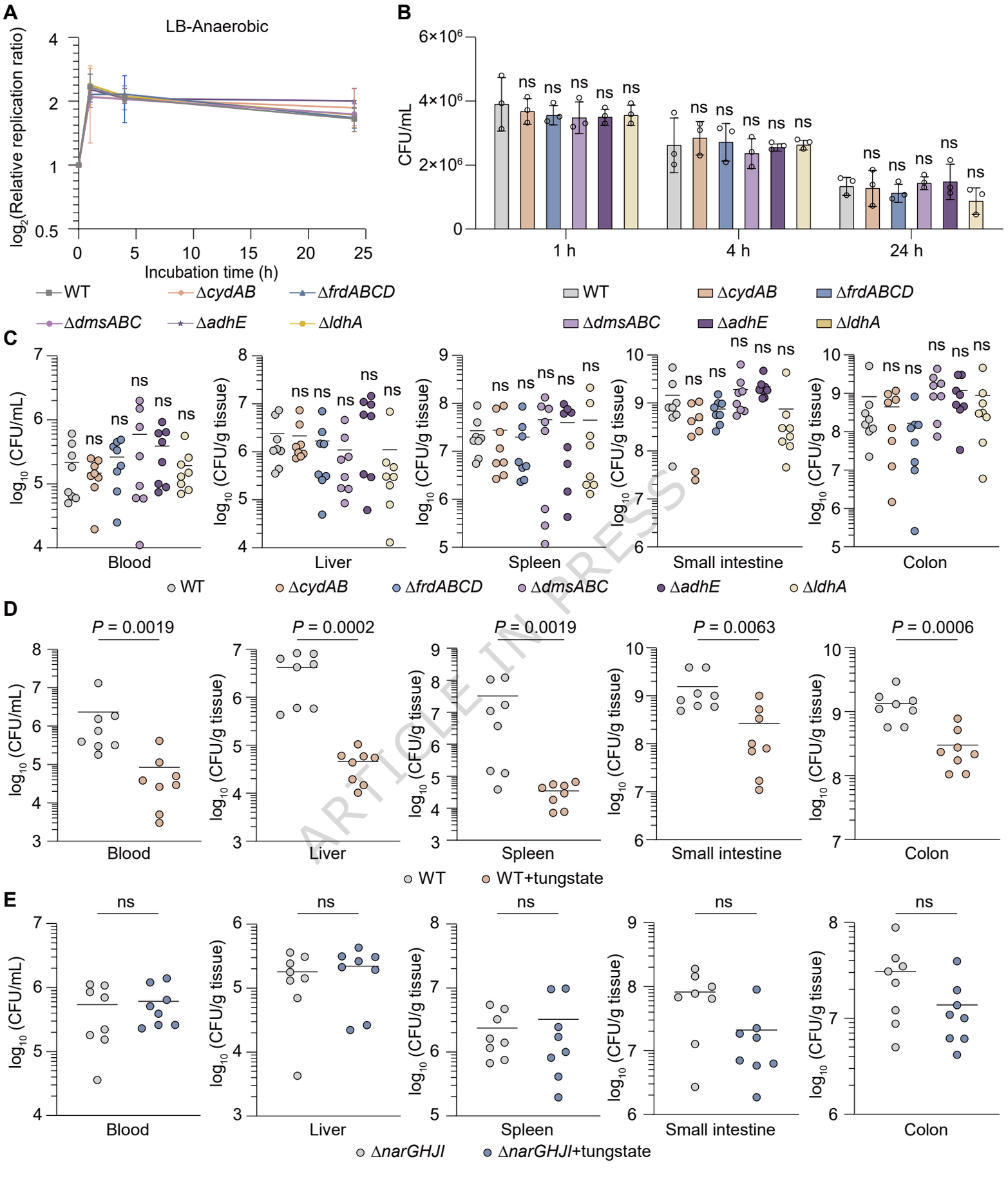

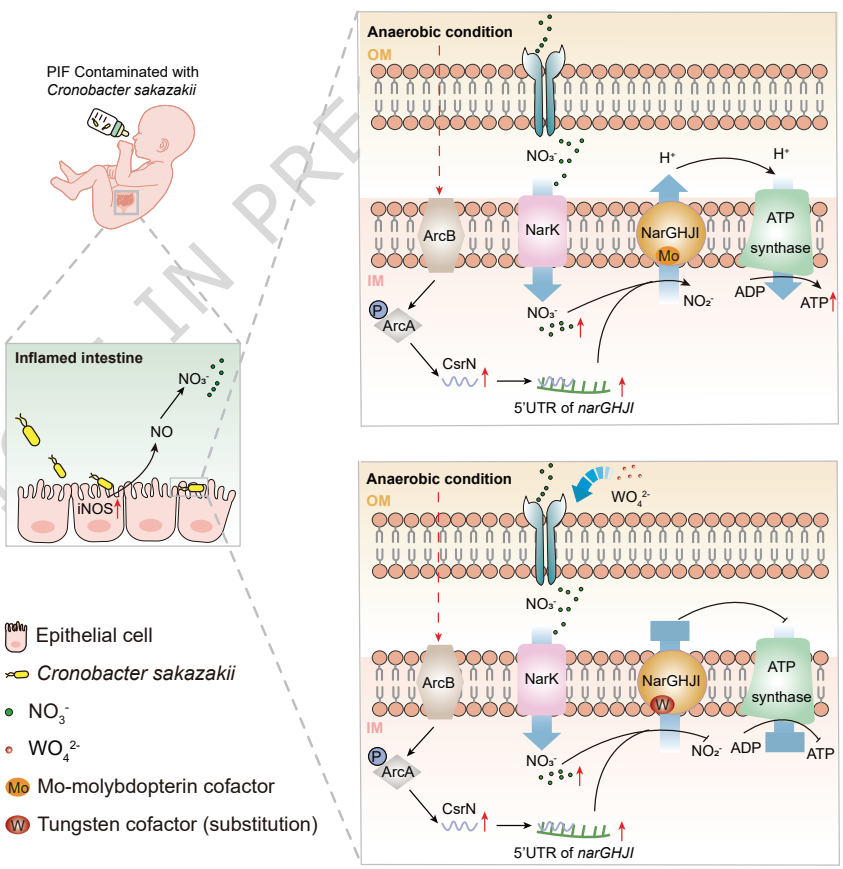
PIF Contaminated with
Cronobacter sakazakii
Inflamed intestine
NO3-
NO
iNOS
Anaerobic condition
OM
IM
NO3-
H+
H+
ArcB
NarK
NarGHJI
Mo
ATP
synthase
NO3-
NO2-
ADP
ATP
P
ArcA
CsrN
5'UTR of narGHJI
Anaerobic condition
WO4 2-
W
Epithelial cell
Cronobacter sakazakii
NO3-
WO4 2-
Mo Mo-molybdopterin cofactor
W Tungsten cofactor (substitution)